Configurational entropy and its crisis in metastable states: Ideal glass transition in a dimer model as a paragidm of a molecular glass

F. Semerianov and P. D. Gujrati*
Department of Physics, Department of Polymer Science, The University of Akron, Akron, Ohio 44311, USA
(Received 15 October 2004; published 7 July 2005)

We discuss the need for discretization to evaluate the configurational entropy in a general model. We also discuss the prescription using restricted partition function formalism to study the stationary limit of metastable states where a more stable equilibrium state exists. We introduce a lattice model of dimers as a paradigm of molecular fluid and study stationary metastability in it to investigate the root cause of glassy behavior. We demonstrate the existence of entropy crisis in metastable states, from which it follows that the entropy crisis is the root cause underlying the ideal glass transition in systems with particles of all sizes. The orientational interactions in the model control the nature of the liquid-liquid transition observed in recent years in molecular glasses.

DOI: 10.1103/PhysRevE.72.011102 PACS number(s): 05.20.−y, 78.55.Qr, 64.70.Pf

I. INTRODUCTION

Glass transition (GT) in a glass-forming system such as a single-component liquid (for example, water and silicate melts) remains a controversial long-standing problem, even after many decades of active investigation and presents one of the most challenging problems in theoretical physics [1–4]. In particular, the existence of high and low density forms of viscous water [5] is a consequence of a liquid-liquid transition in the glassy state [6]. As the liquid is cooled below its melting temperature T_M with sufficient care so that the crystallization does not occur, the liquid gets in a metastable liquid state, commonly known as the supercooled liquid (SCL) state, which is *disordered* with respect to its *ordered* crystalline phase (CR). The glass transition occurs in SCL at a temperature T_G, which is usually about two-thirds of the melting temperature T_M for the liquid. The relaxation time and the viscosity increase by several orders of magnitudes, typically within a range of a few decades of the temperature as it is lowered, and eventually surpass experimental limits. In other words, the system basically freezes at T_G *without* any anomalous changes in its thermodynamic densities like its specific volume or the entropy density. In particular, no spatial correlation length has been identified so far that would diverge near the transition at T_G. On the other hand, mode-coupling theory [7] shows a dynamic slowdown at a temperature T_{MC} much higher than T_G but lower than T_M, and a loss of ergodicity. The relationship between T_{MC} and T_G is not understood at present, although attempts have been made recently [8–10] to understand it partially in connection with long polymers. The free volume falls rapidly near T_{MC} for long polymer fluids, with the nature of the drop becoming singular in the limit of infinitely long polymers. The ideal glass transition occurs at a temperature $T_K < T_{MC}$ where the configurational entropy vanishes, even if the polymer liquid is incompressible [8] at all temperatures. The *configurational entropy* $S(T)$ is defined here, see for example [3], as the entropy that appears in the *configurational partition function* (PF)

$$Z(T) \equiv \frac{1}{v_0^N} \int' e^{-\beta E} d^N\{\mathbf{r}\}, \tag{1}$$

in the canonical ensemble for a system of N particles in a volume V at a given temperature T. The prime indicates that the integration is over distinct configurations, $E(\{\mathbf{r}_i\})$ represents the potential energy in a given configuration $\{\mathbf{r}_i\}$ determined by the instantaneous positions of all the particles, $d^N\{\mathbf{r}\}$ represent integrations with respect to N positions $\mathbf{r}_i$ of the particles, and $\beta \equiv 1/T$, T being the inverse temperature in the units of the Boltzmann constant k_B. The constant v_0 represents some small-scale volume, such as the hard-core volume of a particle, and is introduced here to ensure that $Z(T)$ is dimensionless. Similarly, let ϵ_0 represent some energy constant, such as the average spacing between the energy levels of a single particle in the two-body potential which determines the potential enertgy E of the system. The number of distinct configurations $W(E)dE/\epsilon_0$ with energy in the range E and $E+dE$ determines the *microcanonical* configurational entropy $S(E) \equiv \ln W(E)dE/\epsilon_0 \simeq \ln W(E)$ [11] in the corresponding microcanonical ensemble at a given configurational energy E. For the state to be realizable in Nature, it is obvious that the number of states must be a positive integer. Hence, we must always have $S(E) \geqslant 0$. The average energy $\bar{E}(T)$ in the *canonical* ensemble gives the *canonical* configurational entropy $S(T) \equiv S[\bar{E}(T)]$ in that ensemble, and must also be non-negative. As we will see below, this entropy differs from the total entropy $S_T(T)$ of the system, see (11), which is the entropy associated with the total PF $Z_T(T)$ in (5) below.

A. Kauzmann entropy crisis: A new perspective

The loss of configurational entropy seems to be a generic phenomenon. The thermal data for various systems capable to form glassy states exhibit an *entropy crisis* discovered by

*Electronic address: pdg@arjun.physics.uakron.edu

Kauzmann [1], in which a rapid drop in the *extrapolated entropy* to a *negative* value occurs below the glass transition temperature in SCL [1–4]. This strongly suggests a deep connection between thermodynamics and GT, since thermodynamics requires the entropy to decrease as the temperature is lowered. Consequently, it is tempting to treat the experimentally observed GT as a manifestation of an underlying thermodynamic *ideal glass transition*, which is invoked to avoid the genuine entropy crisis. Kauzmann [1–4] had proposed that the entropy crisis occurs when the excess entropy $S_{ex}(T)$ becomes negative. However, it has become clear that there is no thermodynamic requirement to forbid negative $S_{ex}(T)$ [12]. Thus, in this work, we will instead use the violation of the thermodynamic requirement $S(T) \geqslant 0$ as the signal of the entropy crisis [12] and still attribute it to Kauzmann to honor his pioneering contribution in the field, knowing well that the term is customarily used in a different sense $[S_{ex}(T) < 0]$. This distinction should not be forgotten in this work.

For the metastable SCL, the Kauzmann entropy crisis condition reduces to the SCL *configurational entropy* becoming *negative* ($S_{SCL} < 0$) below a nonzero temperature $T = T_K$: Negative S_{SCL} implies that such states are *unrealizable* in Nature [8–10,13]. Free volume, which also seems to decrease with lowering the temperature [1–4], does not seem to be the primary cause, though it may be secondary, behind GT as shown recently [10], as there is no thermodynamic requirement for it to decrease with the lowering of the temperature.

The entropy crisis and the resulting ideal GT have *only* been substantiated so far in two exact calculations. The first one is an exact calculation by Derrida on an abstract model known as the random energy model [14]. The second one is an explicit exact calculation by Gujrati and coworkers [8–10] in long semiflexible polymers, which not only satisfies the rigorous Gujrati-Goldstein free energy upper bound [15] for the equilibrium state, but also yields $S_{SCL}(T) < 0$ below a positive temperature $T = T_K$ [12]. An earlier demonstration of the crisis in polymers by Gibbs and DiMarzio [16] was severely criticized by Gujrati and Goldstein [15] for its poor approximation that violates the rigorous Gujrati-Goldstein bounds, thus raising doubts about their primary conclusion of demonstrating an entropy crisis [12]. Despite its limitation, the work has played a pivotal role in elevating the Kauzmann entropy crisis from a mere curious observation to probably the most important mechanism behind the glass transition, even though the demonstration was only for long molecules. Unfortunately, the criticism by Gujrati and Goldstein has been incorrectly interpreted by some workers [17] by taking their bounds to be also applicable to the metastable states in polymers. To overcome the bounds, DiMarzio and Yang have suggested to replace the unrealizability condition $S_{SCL} < 0$ by an arbitrary condition $S_{SCL} < S_{c0}$ for the entropy crisis, where S_{c0} is some small critical value [12]. This is not the correct interpretation of the Gujrati-Goldstein bounds. These bounds are only for the equilibrium states, since they are obtained by considering Gujrati-Goldstein excitations in CR; they are not applicable to SCL, which represents a disordered state.

A glass can be thought as a disordered or amorphous solid [18]. There are no general arguments [18,19] to show that thermodynamically stable states must always be ordered, i.e., periodic. The remarkable aperiodic Penrose tilings of the plane, for example, by two differently but suitably shaped tiles are stable. Nevertheless, it appears that most amorphous states in systems that crystallize have much *higher* internal energy or enthalpy than that of the corresponding crystal, even near or at absolute zero [1,18]. Thus, we will consider amorphous solids, i.e., glasses, as representing metastable, rather than stable states in this work. The higher energy of the glass implies [13] a non-zero *ideal glass temperature* (also called here the *Kauzmann temperature*; see [12]) T_K below which the *extrapolated* configurational entropy of the disordered or the amorphous state of the system becomes negative.

It should be stressed that the glass transition is ubiquitous and is also seen in small molecules. Therefore, it is widely believed that the entropy crisis also occurs in molecular liquids. However, no such entropy crisis has ever been demonstrated in any explicit calculation for small molecules [4]. This is highly disconcerting and casts doubts on the importance of the entropy crisis for GT in systems consisting of particles of any size. It is this lack of explicit demonstration of the entropy crisis in molecular liquids that has motivated this work.

There is a clear need to settle whether the entropy crisis is generic for molecules of all sizes. An explicit calculation without any uncontrollable approximation such as an exact calculation for small molecules will go a long way to settle the matter once for all. Without such a calculation, our understanding of GT *cannot* become complete. An exact calculation demonstrating a positive Kauzmann temperature for small molecular fluids would be a major accomplishment. The other motivation for the work is to carefully define the configurational entropy so that is satisfies $S(T) \geqslant 0$ for states that are realizable in Nature. Its *violation* is then argued as a trigger for the glass transition [12].

Our aim here is to fill this gap in our understanding by demonstrating the existence of an entropy crisis in an explicit *exact calculation* on a system of classical dimers as a paradigm of a molecular liquid. In conjunction with our earlier demonstration of the entropy crisis in infinitely and also very long polymer system, our calculation, thus, finally enshrines the Kauzmann entropy crisis [in the sense adopted here [12] that a negative S_{SCL}, and not a negative $S_{ex}(T)$, implies that such states are *unrealizable* in Nature] as the general underlying thermodynamic driving force for GT in molecules of all sizes. It should be stated that recent computer simulations have not been able to settle the issue clearly [20]. Our investigation also enables us to draw important conclusions about the role orientational order plays in liquid-liquid phase transitions that have been observed recently in many atomic and molecular liquids [21,22]. It has gradually become apparent that the short-ranged orientational order in supercooled liquids plays an important role not only in the formation of glasses but also in giving rise to a liquid-liquid phase transition. Tanaka [23] has proposed a general view in terms of cooperative medium-ranged bond ordering to describe liquid-liquid transitions, based on the original work of Nelson [24]. Thus, we will also consider orientational order in this work.

It is fair to say that there yet exists no completely satisfying theory of the glass transition [3,4,25] even though some major progress has been made recently [8–10,13,26–30]. Theoretical investigations mainly utilize two different approaches, which are based either on thermodynamic or on kinetic ideas. The two approaches provide an interesting duality in the liquid-glass transition, neither of which seems complete. We discuss below briefly some of the most promising theories based on these approaches.

B. Free volume theory

The most successful theory that attempts to describe *both* aspects with some respectable success is based on the "free-volume" model of Cohen and Turnbull [31]. The concept of free volume has been an intriguing one that pervades throughout physics but its consequences and relevance are not well understood [32], at least in our opinion, especially because there is no consensus on what various workers mean by free volume. Nevertheless, GT in this theory occurs when the free volume becomes sufficiently *small* to impede the mobility of the molecules [33]. The time dependence of the free-volume redistribution, determined by the energy barriers encountered during redistribution, provides a *kinetic* view of the transition, and must be properly accounted for. This approach is yet to be completed to satisfaction. Nevertheless, assuming that the change in free volume is proportional to the difference in the temperature $T-T_{\mathrm{V}}$ near the temperature T_{V}, even though there is no thermodynamic requirement for the free volume to drop as T is lowered [10], the viscosity $\eta(T)$ diverges near T_V according to the Vogel-Tammann-Fulcher equation

$$\ln \eta(T) = A_{\mathrm{VTF}} + B_{\mathrm{VTF}}/(T - T_{\mathrm{V}}), \tag{2}$$

where A_{VTF} and B_{VTF} are system-dependent constants. This situation should be contrasted with the fact that there are theoretical models [8,9,14] *without* any free volume in which the ideal glass transition occurs due to the entropy crisis at a positive temperature. Hence, it appears likely that the free volume itself is not the determining cause for the glass transition in supercooled liquids. However, too much free volume can destroy the transition [10]. We will, thus, explore the influence of free volume on the glass transition in this work.

C. Thermodynamic theory

The thermodynamic ideas alone describe GT in terms of the *entropy crisis*, when the extrapolated entropy $S(T)<0$ at a positive temperature [12], so that there occurs a rapid entropy drop to a *negative* value below the glass transition temperature in the supercooled liquid (SCL) [1–4]. An *ideal glass transition* at T_{K} is invoked to avoid the entropy crisis [12]. The entropic view plays a central role in the Adams-Gibbs theory [34], according to which the viscosity $\eta(T)$ above the glass transition depends on a quantity which, though not clearly defined, is also called the configurational entropy. This entropy is denoted by $S_{\mathrm{conf}}(T)$ so as not to be confused with our configurational entropy $S(T)$. In terms of $S_{\mathrm{conf}}(T)$, the viscosity is given as follows:

$$\ln \eta(T) = A_{\mathrm{AG}} + B_{\mathrm{AG}}/TS_{\mathrm{conf}}(T), \tag{3}$$

where A_{AG} and B_{AG} are system-dependent constants. The existence of the entropy crisis has been justified in many exact model calculations [8–10,14,16]. An alternative thermodynamic theory for the impending entropy crisis based on spin-glass ideas has also been developed in which proximity to an underlying first-order transition is used to explain the glass transition [26].

In a thermodynamic theory, the glass-forming system is treated as homogeneous, mainly because there appears to be no evidence of any structural changes emerging near GT. From this point of view, a thermodynamic theory gives rise to a homogeneous free energy. However, the fluctuations in it can be used to construct the equations for time dependence in the system. Thus, the thermodynamic approach can be used to describe the dual aspect of the glass transition. In particular, it should enable us to provide a bridge between the two expressions in (2) and (3) for the viscosity that are the most widely-used and successful formalism of viscosity in glass-forming liquids.

D. Mode-coupling theory

The mode-coupling theory [7] is an example of theories based on kinetic ideas in which glass formation is described as a slowing down of liquid's mobility and its freezing into a unique amorphous configuration at a positive temperature. In this theory, the ergodicity is lost completely, and structural arrest occurs at a temperature T_{MC}, which lies well above the customary glass transition temperature T_{G}. Consequently, the correlation time and the viscosity diverge due to the *caging effect*. The diverging viscosity can be related to the vanishing free volume [31,33], which might suggest that *the MC transition is the same as the glass transition*. This does not seem to be the consensus at present. Thus, it is not clear if the free volume is crucial for the MC transition. Some progress has been made in this direction recently [10], where it has been shown for long polymers that the free volume vanishes at a temperature much higher than the ideal glass transition. The mode-coupling theory is also not well understood, especially below the glass transition. More recently, it has been argued that this and mean-field theories based on an underlying first-order transition may be incapable of explaining dynamic heterogeneities.

E. Theory vs experiment and simulation

In this work, we are interested in the thermodynamic approach to investigate the entropy crisis, according to which the configurational entropy $S_{\mathrm{SCL}}(T)$ vanishes at some positive temperature [12]. It should be remarked that the entropy crisis can only be seen in theoretical calculations, but never in an experiment or simulation, since the latter two always deal with states that are observed or produced, so that the corresponding entropy would never be negative. It is only by extrapolation that the latter two may predict an entropy crisis. The reliability of such extrapolation is debatable, and has been used to argue against an entropy crisis [35,36]. By analyzing experimental data, they have argued on procedural

grounds that an entropy crisis in any experiment must be absent, which we agree with. However, such arguments based solely on experimental data or simulation *without extrapolation* can never shed light on the issue of the entropy crisis, which is purely hypothetical. To verify the existence or nonexistence of the crisis, one must resort to theoretical arguments. Several workers [37,38] have argued theoretically that it is not possible to have any entropy crisis, not withstanding the explicit demonstration of it in long polymers, and in the abstract random energy model. The argument due to Stillinger [37], in particular, is forceful though not rigorous [4]. While he concedes that long polymers may very well have an entropy crisis at a positive temperature, he argues for its absence in viscous liquids of small molecules. From a purely mathematical point of view, it is hard to understand how this scenario could be possible. Using the physical argument of continuity, we expect T_K to be a smooth function of the molecular weight. Thus, it does not seem possible that such a function remains zero over a wide but finite range of the size of the molecules, and abruptly becomes nonzero for very large sizes. A function like this must be a singular function. However, no argument that we can imagine can support a particular large molecular size to play the role of the location of such a singularity.

Assuming the entropy in (3) to be the configurational entropy, which is known to vanish in theoretical calculations, its rapid decrease to zero should give rise to a diverging viscosity, thus providing a connection between the thermodynamic view and the kinetic view. However, no experimental evidence in support of such a diverging viscosity is known mainly because the relaxation times become much longer than the experimental time limitations. Thus, it should not be surprising that theoretical predictions of entropy crisis is never going to be seen directly in experiments.

Despite this, the suggestion that the rapid rise in the viscosity is due to a sudden drop in $S(T)$ seems very enticing, since both phenomena are ubiquitous in glassy states. The experimental data indicate that T_V and T_K are, in fact, very close [39], clearly pointing to a close relationship between the rapid rise in the viscosity and the entropy crisis. This deep connection, if true, provides a very clean reflection of the dual aspects of the glassy behavior mentioned above. It also implies strongly that it is the entropy crisis, which is the root cause of the glass transition. This idea got a strong support recently when it was shown that the free volume could not be the root cause for GT in SCL, as the transition can exist even in the absence of the free volume [10]. Thus, we are driven to the conclusion that it should be possible to treat the SCL glass transition within a thermodynamics formalism by demonstrating the existence of the entropy crisis. In other words, if the scenario is valid, we can treat the experimentally observed GT as a manifestation of the underlying ideal glass transition induced by the entropy crisis. The ideal glass transition is a hypothetical transition obtained in the limit of infinite slow cooling, provided the crystal (CR) is forbidden to nucleate. This transition will never be observed in experiments since such cooling rates are impossible to maintain in reality or in simulations since any state generated in simulation will ensure that the entropy is not negative. Thus, experimentally or in simulations, one would never observe the ideal glass transition directly. It can only be inferred either by some sort of extrapolation or by diverging relaxation times in these methods. On the other hand, a theoretical demonstration of an ideal glass transition is possible since neither the time restriction is an issue nor the realizability of a state. The theoretical existence of an ideal glass transition forces us to conclude that the observed glass transitions in experiments are a manifestation of this transition, or in other words, of the entropy crisis. As such, a study of the glass transition within a thermodynamics formalism will enable us to understand glassy phenomena in a systematic and fundamental way.

It should be noted that what one measures in experiments is the difference in the entropy, and not the absolute entropy. Assuming that the entropy is zero at absolute zero in accordance with the Nernst-Planck postulate, one can then determine the absolute entropy experimentally. However, it is well known that SCL is a metastable state, and there is no reason for its entropy to vanish at absolute zero [18]. Indeed, it has been demonstrated some time ago that the residual entropy at absolute zero obtained by extrapolation is a nonzero fraction of the entropy of melting [40], which is not known *á priori*. Therefore, it is *impossible* to argue from experimental data that the entropy indeed falls to zero, since such a demonstration will certainly require calculating absolute entropy though efforts continue to this date [35,36].

The layout of the paper is the following. In the next section, we discuss classical statistical mechanical approach to study glass transition and show the need for discretizing both the real and the momentum spaces. We also compare the configurational entropy in (1) and the criterion for the entropy crisis with other definitions and criteria available in the literature. In Sec. III, we describe the classical dimer model, and its Husimi cactus approximation is discussed in Sec. IV. We solve the model exactly on the cactus by using the recursion relation (RR) technique and the results are presented in Sec. V. The final section contains discussion of our results and conclusions. The RR's are deferred to the Appendix.

II. CONFIGURATIONAL PARTITION FUNCTION AND ENTROPY CRISIS

A. Negative entropy in continuum classical statistical mechanics

We consider a system of N identical particles $i=1,2,\ldots,N$ confined in a container of volume V. The position $\mathbf{r}_i$ and momentum $\mathbf{p}_i$ of the particle i are treated as continuous variables in classical mechanics. The Hamiltonian of the system is given by

$$H \equiv \sum_i \mathbf{p}_i^2/2m + E(\{\mathbf{r}_i\}). \tag{4}$$

The first term in (4) represents the kinetic energy K. In classical statistical mechanics (CSM), the total partition function (PF) Z_T for the system can be reduced to a product of two different dimensionless integrals as

$$Z_T(T) \equiv Z_{KE}(T)Z(T), \tag{5}$$

where

$$Z_{\mathrm{KE}}(T) \equiv \frac{v_0^N}{(2\pi\hbar)^{3N}} \int e^{-\beta K} d^N\{\mathbf{p}\} \tag{6}$$

denotes the PF due to the translational degrees of freedom in which $d^N\{\mathbf{p}\}$ represents integrations with respect to N momenta $\mathbf{p}_i$ of the particles. The prefactor in terms of $\hbar$ is used not only to make Z_{T} dimensionless, but also to explicitly show the correspondence of Z_{T} with the corresponding PF in the quantum statistical mechanics (QSM) in the classical limit $\hbar \to 0$. Despite the classical limit requirement $\hbar \to 0$, we are not allowed to set $\hbar = 0$ in the final result, but keep its actual nonzero value. Accordingly, some problems remain such as Wigner's distribution function not being a classical probability distribution, which we do not discuss any further but refer the reader to the literature [41]. Keeping $\hbar$ at its nonzero value avoids infinities as we will see below but in no way implies that we are dealing with quantum effects. In particular, it does not imply that the entropy is non-negative, as can be seen in the following. The PF Z_{KE} can be written in terms of $W_{\mathrm{KE}}(P)dP \equiv C_{3N} v_0^N P^{3N-1} dP/h^{3N}$, which is usually thought of as representing the *number of microstates* corresponding to the magnitude of the total momentum P in the range P, and $P+dP$ in the $3N$-dimensional momentum space, as follows:

$$Z_{\mathrm{KE}} \equiv \int W_{\mathrm{KE}}(P) e^{-\beta K} dP. \tag{7}$$

Here $C_D \equiv D\pi^{D/2}/\Gamma(D/2+1)$ is a constant arising from the angular integration in a $(D=3N)$-dimensional space. Being a number of states, $W_{\mathrm{KE}}(P)dP$ should be a *positive* integer, which as we see below is not true. The entropy function due to kinetic energy $K \equiv P^2/2m$ is given by $S_{\mathrm{KE}} = \ln W_{\mathrm{KE}}(P)$ [11]. In the thermodynamic limit $N \to \infty$, the integrand in (7) must be maximum. Hence, we look for the maximum of $P^{3N-1} e^{-\beta K}$ by the prescription, known commonly as the saddle point approximation, of equating its derivative to zero. This immediately gives the ideal gas equation for the average kinetic energy $\bar{K}(T)$

$$\bar{K}(T) = (3/2)NT, \tag{8}$$

which should come as no surprise. For the ideal gas, the total entropy function $S_{\mathrm{T}}(T)$ is given by

$$S_{\mathrm{T}}(T) = N \ln(Ve/\lambda^3 N), \tag{9}$$

in terms of a $\lambda \equiv h/\sqrt{2\pi meT}$, a quantity related to the de Broglie thermal wavelength. This entropy is independent of the choice of v_0, while

$$S_{\mathrm{KE}}(T) = N \ln(v_0/\lambda^3) \tag{10}$$

depends on v_0. However, it should be noted that $S_{\mathrm{KE}}(T)$ has the *same* value at a given temperature for any classical system, regardless of the configurational energy, provided v_0 is common to all of them. It is most certainly the same for all phases of any system. Thus, in general, the configurational entropy can be always obtained by subtracting $S_{\mathrm{KE}}(T)$ from $S_{\mathrm{T}}(T)$ [10]:

$$S(T) \equiv S_{\mathrm{T}}(T) - S_{\mathrm{KE}}(T). \tag{11}$$

For an ideal gas, the configurational PF is $Z = (V/v_0)^N/N!$, and the corresponding configurational entropy, which no longer depends on T, is

$$S = N \ln(Ve/v_0 N). \tag{12}$$

All these entropies are extensive, as expected. If we set $h=0$, we encounter an infinity in the entropy at all temperatures in (10). To avoid this, we keep h at its nonzero value.

At very low temperatures ($\lambda^3 \gg v_0$), or for high densities ($V/v_0 N \ll 1/e$), S_{T} becomes negative and eventually $S_{\mathrm{T}} \to -\infty$, a well-known result of classical statistical mechanics. We also note that for $V/v_0 N < 1/e$, the configurational entropy S in (12) also becomes negative and eventually diverge to $-\infty$. [A similar behavior is also seen in $S_{\mathrm{KE}}(T)$ for low T.] It appears at first glance that the problem is due to the pointlike nature of the particles, which allows us to pack as many particles as we wish in a given fixed volume V. This is not true. The problem is due to the continuum nature of the real space. This is easily seen from the exact solution of the 1D Tonks gas, which is a simple model of noninteracting hard rods, each of length l. In one dimension, we will take v_0 to have the dimension of length. The configurational entropy S corresponding to N rods in a line segment of length L is given by [42]

$$S = N \ln[(L - Nl)e/v_0 N] \tag{13}$$

in the thermodynamic limit, while S_{KE} is given by the 1D analog

$$S_{\mathrm{KE}}(T) = N \ln(v_0/\lambda)$$

of (10), where m now represents the mass of a rod. Comparison with (12) shows that the only difference is that the total volume V in (12) is replaced by the free volume analog $L - Nl$ for the 1-dimensional Tonks gas; see (13). It is clear that the entropy becomes *negative* as soon as $L/v_0 N < 1/e + l/v_0$ and eventually diverges to $-\infty$ in the fully packed state. Similarly, the problem with $S_{\mathrm{KE}}(T) \to -\infty$ as $T \to 0$ is due to the continuum nature of the momentum space.

For the choice $v_0 = l$, the condition for negative configurational entropy becomes $L/Nl < 1 + 1/e$. This condition will change as we make another choice of v_0. However, it should be stated that the arbitrariness in the definition of the configurational entropy due to the presence of v_0 is no different than the arbitrariness due to the units of length or volume that is present in the configurational entropy, when one does not use v_0 to make the configurational PF dimensionless. This is the case investigated in [42] where $Z(T)$ has the dimensions of $(\text{length})^N$. Correspondingly, the entropy is no longer a pure number, and has the value

$$S = N \ln[(L - Nl)e/N],$$

which differs from the above entropy (13) in that v_0 is absent. It is clear that the value of this entropy changes with the units of length one uses to measure the length L of the system. In our approach, this arbitrariness is reflected in the presence of v_0; see also Sec. II C below for more on this issue.

It is clear that $S_T(T)$ remains independent of v_0. But the issue of a negative $S_T(T)$ persists as discussed above. This problem disappears as soon as we invoke quantum statistical mechanics to describe the total PF, which no longer can be written as product of two or more PF's as in (5), and we need to consider $S_T(T)$. Thus, we need to consider the number of states $W_T(E_T) \geq 1$ as function of the (total) energy eigenvalue E_T. The energy eigenvalue E_T can certainly be broken into the kinetic energy part K and the potential energy part E, but such a partition is not possible for the total entropy $S_T \equiv \ln W_T(E_T)$. Therefore, in general, the notion of the configurational entropy does not make sense in this case. Since we are only concerned with classical statistical mechanics in this work, we will not discuss this point further here.

B. Partitioning of $Z_T(T)$

An important comment about the form of the potential energy E in (1) and the partitioning in (5) is in order. We have implicitly assumed that the potential energy contains all physical interactions, and that no interaction depends on velocities. This restriction means that, for example, we do not consider magnetic interactions. This is not a major limitation as this case covers a majority of the cases. The existence of these interaction potentials means that we only deal with conservative forces. The potential energy of the system must certainly include the interaction energy that would be responsible for strong chemical bondings, such as in a polymer, if they occur in the system (below some temperature). This approach allows us to describe the vibrational modes associated with chemical bonds also. However, the most important reason to use this approach is to be able to treat all $3N$ Cartesian degrees of freedom (due to $3N$ coordinates $\{\mathbf{r}_i\}$) as independent. If, however, we treat the chemical bonds as fixed in length, this reduces the degrees of freedom due to these holonomic constraints that do not depend on time and temperature. This does not create any complication, as can be seen from the following argument. The theory of Lagrange multiplier allows us to treat the $3N$ degrees of freedom as independent at the expense of adding forces of constraints [43], which we take to be also conservative since the constraints themselves arise from conservative forces. This modifies the potential energy E by an additional potential energy that is independent of time and temperature, and the partitioning in (5) continues to remains valid. The issue of constraints due to chemical bonds is also studied by Di Marzio [44], but from a different point of view. The potential energy he considers does not involve interactions responsible for bond formation. Thus, his formulation is quite different from ours (but see Sec. VI below also). Our approach allows us to avoid the complications noted by Di Marzio.

In case the potential energy depends on velocities, we can still factor out a PF related to the center-of-mass kinetic energy; the remainder PF will play the role of the configurational PF; however, such a case has never been studied within the context of SCL and glasses and will not be pursued anymore in this work.

C. Non-negative entropy in classical statistical mechanics

As shown above, the entropy of a continuum model is invariably negative in classical statistical mechanics, either at low temperatures or at high densities; but this has nothing to do with the entropy crisis noted by Kauzmann as defined here [12]. Quantum statistical mechanical calculations are not feasible at present to make entropy non-negative. Thus, at present, no theoretical calculation using continuum classical statistical will be able to justify the entropy crisis, as the negative entropy may just be a manifestation of the continuum picture such as in the random energy model [14]. A lattice picture ensures a non-negative entropy for any state that can be realized in Nature. Thus, a lattice model is capable of settling whether an entropy crisis occurs in the metastable state or not.

To define microstates so that their number is always greater than or equal to 1, one must *discretize* the real and momentum spaces carefully. For this purpose, we introduce a short distance a in real space (we can define it through $v_0 \equiv a^3$), and a related quantity $b \equiv 2\pi\hbar/a$ having the dimension of the momentum in the momentum space, so that $ab = 2\pi\hbar$. (In a lattice model, v_0 will represent the lattice cell volume.) We now divide the two spaces into cells of size a^{3N} and b^{3N}, respectively. In the discretized space, the number of microstates is nothing but the number of distinct ways the cells are occupied by the particles' positions and momenta. This number *cannot* be less than unity if the microstate is realizable in Nature. Hence, the entropy can never be negative if the state occurs in Nature. For example, $C_{3N}P^{3N-1}dP$ is now replaced by the number of cells of size b^{3N} that cover a shell of integer radius $\bar{P}=P/b$, and thickness b (corresponding to the integer thickness $\overline{dP}=dP/b=1$). This number is $C_{3N}\bar{P}^{3N-1}$. The equilibrium is obtained by maximizing the integrand

$$I(\bar{P}) \equiv \bar{P}^{3N-1}e^{-(\beta b^2/2m)\bar{P}^2}.$$

Maximizing I is equivalent to maximizing

$$\tilde{I} \equiv I(\bar{P})/I(1) \equiv \bar{P}^{3N-1}e^{-(\beta b^2/2m)(\bar{P}^2-1)}, \tag{14}$$

in which $\bar{P}^2-1 \geq 0$. It is evident that the maximum of $\tilde{I}$ at $\beta \to \infty$ corresponds to $\bar{P}=1$, and gives $\tilde{I}=1$. This is true for all N, and will remain true even as $N \to \infty$. In this limit, higher values of $\bar{P}$ also condense to the state corresponding to the lowest energy density per particle. Thus, the number of microstates at absolute zero is strictly a positive integer. Correspondingly, the entropy is *not* negative anymore. It is also clear that for small values of $\bar{P}$ (and finite N), we cannot differentiate $\tilde{I}$ with respect to $\bar{P}$ to find the maximum, as $\bar{P}$ cannot be approximated as a continuous variable in this range. Thus, care must be exercised near absolute zero.

A similar conclusion is drawn for the configurational entropy determining Z in (5). It is also easy to see that the total entropy is independent of the choice a or b, though its two components are not. As we will see below, we are mostly interested in the configurational entropy, which from the above is seen to depend on a. This is an unwanted behavior, since it makes $S(T)$ depend on the somewhat arbitrary parameter a. This unwanted property is easily taken care of by expressing the configurational entropy in terms of the dimen-

sionless volumes, lengths, etc. like $\bar{V} \equiv V/a^3$, l/a, etc. In the following, we will always interpret the discretized configurational entropy in this sense.

It is now obvious that the entropy will be non-negative for equilibrium states, since these states occur in Nature. This property need not hold for metastable states, to be properly defined below through analytical continuation of the free energy, for which a negative entropy now will only indicate that the corresponding state represented by the free energy continuation is *not* realizable in Nature; it is no longer a mere consequence of the continuum picture as above. An exact calculation, like the one we carry out in this work, will evaluate the partition function exactly *without* using the saddle-point method. It is the continuation of the resulting free energy that is used as the SCL free energy. Thus, the calculation does not directly identify the metastable states; rather their existence is indirectly inferred from the free energy continuation. It will be seen that the entropy is non-negative for the equilibrium state. We will also see that it can become negative for metastable states. The part of the metastable state with non-negative entropy represents the metastable state that can occur in Nature. Thus we wish to emphasize the following point as a proposition.

Proposition 1. The mathematical existence of the free energy under continuation to indirectly identify metastable states does not necessarily mean the existence of real metastable states that could be observed in Nature.

We will assume in the following that a discretization of the two spaces has been carried out. In particular, a lattice model in which the particle positions are restricted to be on the lattice sites is very useful from this point of view. There is no kinetic energy in the lattice model. Therefore, we can assume that $S_{\mathrm{KE}}(T) \equiv 0$. This leaves us with only the configurational entropy, which represents the entire entropy in the lattice model.

D. Other common definitions of the configurational entropy

It should be clear from the above that the configurational entropy is a concept that can only be introduced in classical statistical mechanics. Unfortunately, there is no direct measurement of the configurational entropy of a system. Thus, its experimental determination is a challenge. There is a further complication in that there is a certain amount of confusion and/or ambiguity about its definition. Our definition in (11) is the most natural definition of the configurational entropy for which the requirement $S(T) \geqslant 0$ can be justified on the ground that the state must be realizable in Nature. We will call this the *thermodynamic principle of reality* [8–10,12,13]. The configurational entropy represents that part of the total entropy $S_{\mathrm{T}}(T)$, which is due to the configurational degrees of freedom only [3]. The remainder of the entropy $S_{\mathrm{KE}}(T)$ is due to the translational degrees of freedom and must be subtracted from the total entropy to obtain $S(T)$. Thus, there is no ambiguity in its definition.

The ambiguity arises when we need to estimate $S(T)$ by subtracting the contribution $S_{\mathrm{KE}}(T)$, see (11), for the following reason. In a solid state like the glass or CR, where the average particle positions are almost fixed, $S_{\mathrm{KE}}(T)$ is a significant part of the total entropy. It represents the part of the vibrational entropy (due to vibrations within a potential well) due to the kinetic energy; we assume that the container is stationary. The other part of the vibrational entropy is due to the potential energy of the well, which may even be anharmonic. The difference in (11) represents the configurational entropy. If no discretization has been carried out, then $S_{\mathrm{KE}}(T)$ is given by (10). This will surely create a problem at low temperatures where $S_{\mathrm{KE}}(T)$ and $S(T)$ become negative. Thus, discretization is necessary, and one needs to carry it out before $S_{\mathrm{KE}}(T)$ can be calculated. In that case, we need to express the discretized configurational entropy $S(T)$ in terms of the dimensionless volume $\bar{V}$ as discussed above.

Traditionally, one treats the translational degrees of freedom approximately in a different fashion, at least for CR. The discretization is enforced by treating the resulting motion as giving rise to quantum vibrations about the minimum of the CR configurational energy. [If we treat these vibrations classically, it can be shown immediately that the kinetic energy contribution to the entropy is precisely given by $S_{\mathrm{KE}}(T)$.] Hence, $S_{\mathrm{KE}}(T)$ differs from the vibrational entropy by an amount exactly equal to the configurational entropy, which need not be small. One further assumes that the vibrational modes of SCL are similar to those in CR. Since it is almost impossible to extract $S_{\mathrm{KE}}(T)$ experimentally, one approximates it by the CR entropy and traditionally defines the SCL configurational entropy by [3]

$$S_{\mathrm{SCL}}(T) \simeq S_{\mathrm{ex}}(T) \equiv S_{\text{T-SCL}}(T) - S_{\text{T-CR}}(T).$$

Some workers identify the SCL configurational entropy by the difference $S_{\text{T-SCL}}(T) - S_{\text{T-GL}}(T)$, the excess SCL entropy over the extrapolated entropy of the corresponding glass [45].

Yet, another definition is also common. Workers using the potential landscape picture use the concept of potential energy basins, and define the configurational entropy to be the entropy of inherent structures of a given potential energy $E(T)$ [37]. A related, but more sensible notion of the configurational entropy, as shown recently [46], is the complexity $\mathcal{S}(T)$, which is determined by the number of basins of the same free energy. Its difference from $S(T)$ is the potential energy part $S_{\mathrm{b}}(T)$ of the vibrational entropy associated with a basin [46]: $S(T) = S_{\mathrm{b}}(T) + \mathcal{S}(T)$. The kinetic energy part of the entropy is precisely given by $S_{\mathrm{KE}}(T)$ as said above.

In this work, we will continue to use $S(T)$ to define the configurational entropy. In a lattice model, which we consider later in this work when we introduce the dimer model, we bypass the complication due to $S_{\mathrm{KE}}(T)$ all together since there is no kinetic energy on a lattice. Hence, the entire entropy in the lattice model is purely configurational. The role of the dimensionless volume $\bar{V}$ is played by the number of lattice sites N_{L}. However, the discussion in the rest of this section is applicable to the general case.

E. Metastability continuation

1. Disordered and ordered PF's

A partitioning of the total PF into two or more PF's in CSM, such as in (5), of decoupled degrees of freedom has an

important consequence, which we discuss below. We focus on (5), but the discussion is valid for any general partitioning. The total entropy is a sum of the entropies from the two PF's. The partitioning implies not only that the total entropy at a given temperature is a sum of the entropy contribution due to Z_{KE} and that due to Z, but also that the two contributions are independent. In particular, $S_{KE}(T)$ remains the same, whether we consider the crystal or the supercooled phase, both of which can exist at the same temperature below T_M. This is because CR and SCL are described by Z, and its appropriate modification to be described below, respectively. Hence, we come to a very important conclusion, which we list as a proposition.

Proposition 2. In classical statistical mechanics, which is what is conventionally used to analyze metastability, the contribution $S_{KE}(T)$ to the total entropy $S_T(T)$ from the translational degrees of freedom is the same for various possible phases like SCL or CR that can exist at a given temperature, and is a function only of the temperature T.

Therefore, from now on, we will only consider the configurational degrees of freedom. Since the heat capacity is non-negative, $S(T)$, and $E(T)$ are monotonic increasing function of T, and must reach their minimum values at absolute zero. Assuming CR to be the stable phase at absolute zero, we conclude that it must be in the state with the lowest possible energy denoted by E_0. We also assume, in accordance with the Nernst-Planck postulate, that $S_{CR}(T=0)=0$, i.e., $W(E_0)=1$. Thus, E_0 *sets the zero of the temperature scale in the system*. All other energies in the system are higher than E_0. As long as the heat capacities of various phases, stable or metastable, remain positive, and we will see that this is true, these higher energies will correspond to temperatures $T>0$. In particular, higher energy $E_K>E_0$ of the ideal glass will imply that the ideal glass appears at a positive temperature $T_K>0$ [13].

At high temperatures ($T>T_M$), the system is an equilibrium liquid (EL). At low temperatures ($T<T_M$), the system is an equilibrium crystal CR. At T_M, the two equilibrium states are at coexistence and have the same free energy. It is customary to distinguish the disordered EL and the ordered CR by the use of the order parameter ρ [44], which is conventionally defined in such a way that $\rho=0$ represents the disordered phase, while $\rho\neq 0$ represents the ordered phase. We will now use the notion of the order parameter to describe the metastable state. We will assume that the metastable state of interest is the one obtained under infinitely slow cooling, but always ensuring that the CR is never allowed to nucleate. We call such a metastable state a *stationary metastable state* (SMS). The most convenient way to describe SMS is by the use of a PF. For this, we need to know the number of those configurations of energy E that yield SMS.

2. Entropy continuation for metastability

We follow the well-established practice of describing these states by imposing the constraint that the configurations must satisfy $\rho=0$ [47]; see also [48]. The number of configurations $W(E)$ for a given energy E can be partitioned into $W_{dis}(E)$ and $W_{ord}(E)$, representing the number of disordered ($\rho=0$) and ordered ($\rho\neq 0$) configurations, respectively. Correspondingly, we have two entropy functions $S_{dis}(E)\equiv \ln W_{dis}(E)$, $S_{ord}(E)\equiv \ln W_{ord}(E)$. At higher energies, $S_{dis}(E)>S_{ord}(E)$. At lower energies, $S_{dis}(E)<S_{ord}(E)$. From what has been said above, we have $S_{ord}(E_0)=0$ for the ideal crystal, which occurs at $T=0$. It is usually the case experimentally that the glass has a higher energy than CR at absolute zero. In particular, the ideal glass there has the energy $E=E_K>E_0$. Thus, it appears likely, but not necessary, that $S_{dis}(E_K)=0$. Note that the Nernst-Planck postulate is for equilibrium states. Assuming that E_K is *not* a point of singularity of $S_{dis}(E_K)$, we perform a continuation of $S_{dis}(E)$ to all energies $E\geqslant E_0$, which we also denote by $S_{dis}(E)$, as there will be no confusion. We now use the extended $S_{dis}(E)$, and $S_{ord}(E)$ to construct two configurational PF's $\{W_\alpha(E)\equiv \exp[S_\alpha(E)]\}$

$$Z_\alpha(T)=\sum_{E\geqslant E_0} W_\alpha(E)e^{-\beta E},\quad \alpha=\text{dis,ord}. \tag{15}$$

3. Temperature scale

We also introduce the PF

$$\hat{Z}_{dis}(T)=\sum_{E\geqslant E_K} W_{dis}(E)e^{-\beta E}, \tag{16}$$

related to the disordered configurations, which only uses the unextended entropy function $S_{dis}(E)$, $E\geqslant E_K$. Let us compare $\hat{Z}_{dis}(T)$ and $Z_{dis}(T)$. They only differ in terms containing $E<E_K$. For $E\geqslant E_K$, they have the same entropy function $S_{dis}(E)$. In the thermodynamic limit, both PF's at a given T in the high-temperature regime are dominated by that particular average energy $E=E_{dis}(T)$ at which

$$[\partial S_{dis}(E)/\partial E]_{E=E_{dis}(T)}=\beta.$$

Thus, as long as $E_{dis}(T)\geqslant E_K$, or $T\geqslant T_K$, where T_K is the temperature at which $E_{dis}(T_K)=E_K$, the two PF's $\hat{Z}_{dis}(T)$ and $Z_{dis}(T)$ are identical.

Let us consider $T=T_K$. We can rewrite

$$\hat{Z}_{dis}(T_K)=W_{dis}(E_K)e^{-\beta_K E_K}\left[1+\sum_{E>E_K}\frac{W_{dis}(E)}{W_{dis}(E_K)}e^{-\beta_K\Delta E}\right],$$

where $\Delta E=E-E_K>0$, and $\beta_K=1/T_K$. In the thermodynamic limit, the right-hand side approaches $W_{dis}(E_K)e^{-\beta E_K}$, so that

$$\frac{W_{dis}(E)}{W_{dis}(E_K)}e^{-\beta_K\Delta E}\to 0\quad \text{for } E>E_K. \tag{17}$$

This observation plays an important role for the behavior of $\hat{Z}_{dis}(T)$ for $T<T_K$, as we now show. We rewrite it again as above

$$\hat{Z}_{dis}(T)=W_{dis}(E_K)e^{-\beta E_K}\left[1+\sum_{E>E_K}\frac{W_{dis}(E)}{W_{dis}(E_K)}e^{-\beta\Delta E}\right].$$

Expressing $\beta=\beta_K+\Delta\beta$ in $e^{-\beta\Delta E}$, where $\Delta\beta>0$, we observe that the summand in the above equation vanishes on account

of (17). Thus, $\hat{Z}_{\rm dis}(T)$ reduces to the prefactor in the above equation, and we finally have

$$\hat{F}_{\rm dis}(T) \equiv -T \ln \hat{Z}_{\rm dis}(T) = -T \ln W_{\rm dis}(E_{\rm K}) e^{-\beta E_{\rm K}}$$
$$= (T/T_{\rm K}) \hat{F}_{\rm dis}(T_{\rm K}) + (1 - T/T_{\rm K}) E_{\rm K}.$$

Now we use the fact that $\hat{F}_{\rm dis}(T_{\rm K}) = F_{\rm dis}(T_{\rm K}) = E_{\rm K}$, which follows on account of the observation that $S_{\rm dis}(E_{\rm K}) = 0$. Then, the above equation reduces to

$$\hat{F}_{\rm dis}(T) \equiv E_{\rm K} \quad \text{for } T \leqslant T_{\rm K}. \tag{18}$$

This, as we will see below, describes the *ideal glass* below $T_{\rm K}$. It is an inactive phase that has zero entropy and zero heat capacity.

On the other hand, $Z_{\rm dis}(T)$ behaves very differently below $T_{\rm K}$, because it contains the extended entropy function $S_{\rm dis}(E)$ that exists for all energies $E \geqslant E_0$. Since $E_{\rm K}$ is not known *a priori*, we find it convenient to work with $Z_{\rm dis}(T)$ over the entire temperature range $T \geqslant 0$, recognizing the fact that $Z_{\rm dis}(T) = \hat{Z}_{\rm dis}(T)$ only for $T \geqslant T_{\rm K}$, and that the correct physics is described by $\hat{Z}_{\rm dis}(T)$ and not $Z_{\rm dis}(T)$ below $T_{\rm K}$. Indeed, our calculation method does not allow for imposing the restriction $E \geqslant E_{\rm K}$, even if we somehow can determine $E_{\rm K}$, so the method evaluates $Z_{\rm dis}(T)$ and not $\hat{Z}_{\rm dis}(T)$. Thus, the ideal glass free energy in (18) is deduced only after we discover the entropy crisis in the free energy $F_{\rm dis}(T)$, where it must be imposed by hand.

4. Stability

For a macroscopic system, we have $Z(T) \cong Z_{\rm dis}(T)$ for $T > T_{\rm M}$, and $Z(T) \cong Z_{\rm ord}(T)$ for $T < T_{\rm M}$. We now use the continuation of $Z_{\rm dis}(T)$ below $T_{\rm M}$ to describe SMS, the continuation of EL. We can similarly use the continuation of $Z_{\rm ord}(T)$ above $T_{\rm M}$ to describe the superheated CR above the melting temperature. However, we are not interested in this continuation here. We assume that $W_\alpha(E) \geqslant 0$ in the following. As long as $W_\alpha(E) \geqslant 0$, $Z_\alpha(T)$ is a sum of positive terms. Hence, both PF's will satisfy proper convexity properties. In particular, both will yield non-negative heat capacity. Thus, we have a thermodynamically valid description of CR and SMS at low temperatures.

As said above, E_0 sets the zero of the temperature scale. The assumption that $S_{\rm dis}(E)$ is nonsingular at $E_{\rm K}$ has allowed us to continue $S_{\rm dis}(E)$ to all energies $E \geqslant E_0$, so that the same zero of the scale is common to both PF's in (15). [The fact that both states have the same common temperature $T_{\rm M}$ at the coexistence where $Z_{\rm dis}(T_{\rm M}) = Z_{\rm ord}(T_{\rm M})$ does not depend on this continuation, since $Z_{\rm dis}(T) = \hat{Z}_{\rm dis}(T)$ at $T_{\rm M}$.] Our calculation here will show that $S_{\rm dis}(E)$ is indeed nonsingular at $E_{\rm K}$ and its slope becomes infinitely large at E_0. The latter result is very important in that it shows that SMS cannot be treated divorced from CR; both are required for enforcing a proper and common temperature scale.

F. Ideal glass

For states to be observed in Nature, we require the number of microstates in each PF in (15) not to be less than one: $W_\alpha(E) \geqslant 1$. For CR, which we know must exist in Nature, we must certainly have $W_{\rm ord}(E) \geqslant 1$. Recall that we have assumed $W_{\rm ord}(E_0) = 1$.

However, whether the entropies are non-negative is a separate requirement, independent of the convexity properties. It is possible to have non-negative heat capacity even if the entropy is negative. It is highly plausible from our discussion above that $W_{\rm dis}(E) < 1$ for SMS for $E < E_{\rm K}$. Recall that it is likely that $W_{\rm dis}(E) = 1$ at $E_{\rm K}$, and must continue to decrease as E decreases due to non-negative heat capacity.

Existence of a negative entropy causes no singularity or instability in the corresponding PF. Thus, SMS PF can be continued all the way down to $T = 0$, where the average energy and the free energy both equal E_0. This requires that $TS(T) \to 0$ for all states as $T \to 0$. At some positive temperature $T = T_{\rm K}$, the average energy $E_{\rm SMS}(T) = E_{\rm K}$. Since the SMS has a negative entropy below $T_{\rm K}$, it cannot exist in Nature. Thus, this portion of the SMS free energy $F_{\rm dis}(T)$ below $T_{\rm K}$ is unphysical as noted above and must be discarded and replaced by the *ideal glass* of energy $E = E_{\rm K}$ and zero entropy. This state is described by its constant free energy $\hat{F}_{\rm dis}(T) \equiv E_{\rm K}$ below $T_{\rm K}$; see (18). Its necessity is not indicated by any singularity in $F_{\rm dis}(T)$ at $T_{\rm K}$, but by the additional requirement of realizability condition that $S(T) \geqslant 0$. The ideal glass energy at absolute zero remains $E_{\rm K}$, which must represent a potential energy minimum, just as the CR energy E_0 represents the global potential energy minimum. Thus, at $T = T_{\rm K}$, SMS is trapped in this minimum.

The above discussion can be summarized by the following four statements that are going to be verified during our investigation.

(S1) The zero of the temperature scale is set by the potential energy minimum E_0, and not by other minima like the potential energy minimum $E_{\rm K}$.

(S2) The temperature scale of the disordered phase is also fixed by its coexistence with the ordered phase at the melting temperature, where both phases have common free energy and temperature.

(S3) The energies and free energies of all phases, extended when necessary by continuation without any regard to the entropy crisis, are equal at absolute zero [$TS(T) \to 0$ for all states as $T \to 0$].

(S4) The ideal glass does not emerge directly in the statistical mechanical calculation, but is put in by hand to avoid the entropy crisis.

III. MODEL

We address the issue of the glass transition in molecular fluids by considering a solution of molecules and solvent particles. By a mere change of nomenclature, we can use the same system to explain the behavior of a compressible system by treating the solvent particles as representing voids. The solvents can also be thought of the monomers in which dimers can degrade at high temperatures. We are only going

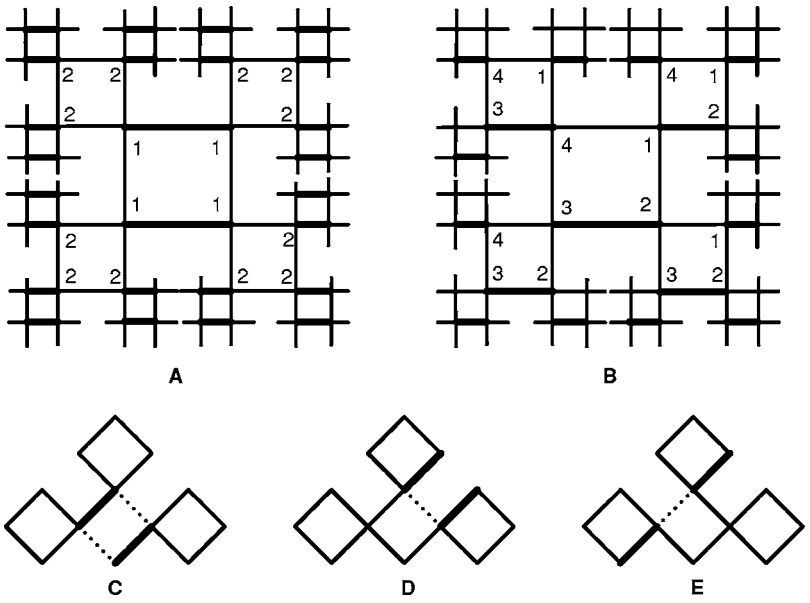

FIG. 1. Columnar (A) and staggered (B) states on Husimi cactus; the labels 1,2,… in (A) and 1–4 in (B), respectively, are introduced to capture the ground states; see description in the text. We show dimers (thick bonds) in the horizontal directions; they can also point in the vertical directions. (C) and (D) show the resonance due to attractive interaction (dotted line) ε_p; (E) shows the axial interaction (dotted line) between collinear dimers.

to consider a lattice model here in which, as shown recently [49], excess or exchange interaction between the solvent particles and the molecules is sufficient to describe orientation-independent mutual interactions on a lattice. This exchange interaction between molecules and solvent particles is usually repulsive. Hence, at low temperatures, there would be phase separation into a molecule-rich phase (a liquid) and molecule-poor phase (a gas). We are only interested in the liquid phase, although our method allows us to capture the solvent-rich phase also. The latter is found to be always unstable. In a lattice model, the ground state should be primarily controlled by the interactions and not by the choice of the lattice; however, the latter may have a secondary influence on the ground state. We wish to minimize the effects of the lattice as much as possible to make our lattice results as useful as possible for a real system. If the molecules are taken as monomeric particles that each occupy a site of the lattice, then such a system is not a suitable candidate for studying glass transition for two reasons. First, their ground state at absolute zero is completely determined by the lattice chosen, since the interactions are no longer present as there are no solvent molecules. The second reason is also very important. Simple liquids with approximately spherical shape and pairwise interactions, such as condensed rare gases or molten alkali halides are very hard to prepare into a viscous liquid state. The simplest means to avoid this is to have anisotropic particles with complex interactions so that the crystalline state is hard to form. This will make it easier to supercool the equilibrium liquid EL below the melting temperature. Dimers are the smallest molecules that (in the absence of any solvent) can get into a unique ordered state not because of the regular lattice structure, but because of physical interactions. Thus, we consider dimers as the simplest molecules to minimize the effects of the lattice on the ordered phase. Furthermore, dimers can also be thought of as representing strongly correlated Cooper pairs in high-T_c superconductors [50].

For the sake of convenience, therefore, we consider a model of classical dimers with solvent on a square lattice, even though other lattices can be considered. The presence of solvent, which can also be treated as void, is not necessary for glass transition as shown recently [10]. Each solvent occupies a site of the lattice. A dimer, on the other hand occupies two consecutive sites and the intervening lattice bond between them. We restrict the excess interaction (energy ε) to a nearest-neighbor pair of a solvent and an endpoint. It is easy to see that there is no one unique ground state at $T=0$. Thus, the mere use of the lattice does not produce an ordered structure, which is very comforting for the reasons stated above. To create a unique ground state to mimic a CR, we need to introduce additional interactions between dimers. These are *orientational interactions* and our model is perfectly suited to investigate the importance of such orientational interactions on the phase diagram.

As the problem cannot be solved exactly on a square lattice, we need to make some approximation. The approximation we make is to replace the regular square lattice by a Husimi cactus, which gives more accurate results than the Bethe lattice approximation [51]. Strictly speaking, there are two perfectly ordered dimer configurations: columnar [Fig. 1(a)] and staggered [Fig. 1(b)]. The problem is thereby subdivided into two separate cases that we study one by one. In order to generate the above mentioned ordered states on the Husimi cactus, two types of interactions between dimer end points are introduced. We associate an interaction energy ε_p for a pair of nearest neighbor end points of two dimers occupying either the same square [Fig. 1(c)] or extending from a given square in a parallel direction [Fig. 1(d)]. If this interaction is attractive, the ground state at $T=0$ is columnar. If the interaction is repulsive, an additional *attractive* axial interaction ε_a between the end points of two collinear dimers [Fig. 1(e)] is introduced so that the ground state at $T=0$ is perfectly ordered staggered phase.

The objective of the present model is not to describe properties of any well known system but to study a generic system showing melting, metastability, and ideal glass transition. The interactions introduced are necessary and, as we will see, also sufficient to achieve perfect order at absolute

zero. Besides, the importance of orientational interactions is acknowledged by now in connection with observed liquid-liquid transitions as well as with the glass transition scenario [21–24]. Such ground states play a central role in the short-ranged resonant valence bond model of high-temperature superconductivity [50], where the pair of parallel dimers are said to resonate; the dimers in Fig. 1(b) are said to anti-resonate. The dimer interactions are induced by quantum fluctuations. Anderson has hypothesized that the columnar phase with resonating dimers is a good representation of pure La_2CuO_4 which is an insulator.

A. Partition function formalism

The rigorous thermodynamic treatment of the model is carried out by using the partition function formalism containing the solvent activity $\eta=\exp(\beta\mu)$, and the Boltzmann weights $w=\exp(-\beta\varepsilon)$, $w_p=\exp(-\beta\varepsilon_p)$ and $w_a=\exp(-\beta\varepsilon_a)$. We consider a lattice containing finite and fixed N_L lattice sites; N_L plays the role of $\bar{V}$. The solvent chemical potential μ is always kept negative ($\mu<0$) to insure a fully dimer-packed ground state at absolute zero. The configurational PF is given as follows:

$$Z=\sum \Omega(N_0,N_p,N_a,N_c)\,\eta^{N_0}w_p^{2N_p}w_a^{N_a}w^{N_c}, \tag{19}$$

where N_0 is the number of the solvent molecules, N_p the number of the resonating dimer pairs, N_a the number of nearest-neighbor axial contacts between the endpoints of collinear dimers, N_c the number of nearest-neighbor solvent-endpoint contacts, and Ω the number of distinct configurations for a given N_0, N_p, N_a, and N_c. The number of endpoint contacts between resonating dimers is twice the number of resonating dimer pairs. The sum is over N_0, N_p, N_a and N_c, consistent with a fixed and finite N_L. The densities in the model, to be denoted by ϕ_k, are defined by the limiting ratios N_k/N_L *per site* as $N_L\to\infty$; here $k=0$, p, a, and c. The ground state at $T=0$ is determined by whether $\varepsilon_p<0$ (attractive) or $\varepsilon_p>0$ (repulsive). For the attractive case, we set $\varepsilon_a=0$ for simplicity, as its presence does not change the topology of the phase diagram.

In the absence of the axial interaction ($\varepsilon_a=0$), the current model is formally related to the model of polydisperse chains studied in [8,9] in the extreme limit when each chain is the shortest possible, a dimer. This requires taking the chain end-point activity $H\to\infty$. However, since it is not possible numerically to handle the limit, we need to study the dimer problem directly, which we do here so that we can also study the effect of the axial interaction.

As shown elsewhere [52], the adimensional free energy

$$\omega=\lim_{N_L\to\infty}(1/N_L)\ln Z$$

represents the osmotic pressure across a membrane permeable to the dimers, but not solvent. The reduced osmotic pressure $\pi_0\equiv Pv_0$ to be also called the pressure in the following for brevity, where v_0 is the volume of a lattice site, is given by

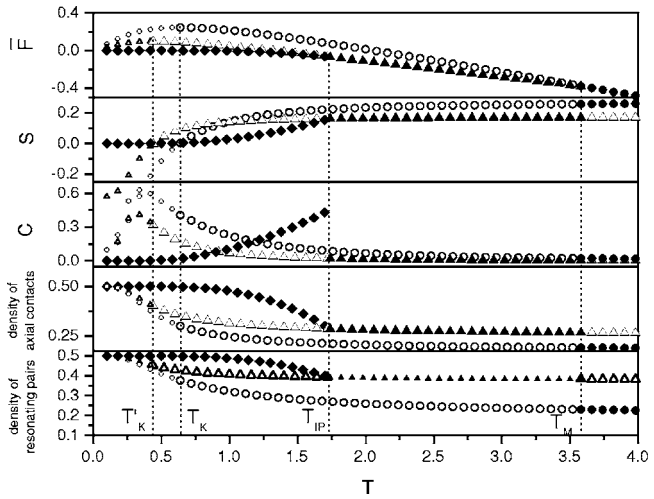

FIG. 2. Temperature dependencies of the shifted thermodynamic potential, the entropy, the configurational specific heat C, and the contact densities ϕ_a and ϕ_p ($\varepsilon_p=-1, \varepsilon_a=0, \eta=0$).

$$\pi_0=T\omega-\mu.$$

The equilibrium state must have the highest pressure among all possible states obtained at given T, w_p, w_a and μ [52]. The energy per site E is given by

$$\beta E=-(2\phi_p\ln w_p+\phi_a\ln w_a+\phi_c\ln w). \tag{20}$$

The entropy per site S is calculated through the Legendre transform of the adimensional pressure:

$$S=\omega+\beta E-\phi_0\ln\eta, \tag{21}$$

where ϕ_0 is the solvent density. Since we are considering a configurational PF, S is purely configurational. (From now on, S and E will represent the configurational entropy and energy per site and not the entropy and energy of the entire system.) At $T=0$, $\phi_c=0$. The maximum value of ϕ_p, ϕ_a is easily seen to be $1/2$ (see Figs. 2 and 5–7).

IV. HUSIMI CACTUS APPROXIMATION

The Husimi cactus is a site-sharing lattice, obtained by connecting two squares or plaquettes at each site so that there are no loops larger than a square are ever formed. An interesting way to think of the relationship between a cactus and a square lattice is to consider the checker-board version of the latter. Then, a cactus can be thought of as approximating the checker-board version of the square lattice in that the cactus only contains squares of a given color [9] of the checker-board, so that the squares of the other color are missing. Husimi cactus incorporates only local loop structure of the regular lattice, but not loops of longer sizes. It is more advantageous than the Bethe lattice as far as the effect of local correlations is concerned, since the Bethe lattice approximation disregards presence of any topological loops. The model is solved *exactly* on the cactus by *recursive technique*, which results in recursion relations (RR's), as shown elsewhere [8–10,53]. The fix-point solutions of the RR's can be classified as 1-cycle, and 2-cycle solutions [8–10], which

will be described in complete detail below. Because of its exactness, the calculation respects (i) all local (such as gauge) and global symmetries, in contrast to the conventional mean-field solution which is known to violate local symmetries, and (ii) thermodynamics is never violated.

This makes the present approach superior to other methods of constructing mean-field solutions based on random mixing approximation [53], because more local correlations are taken into account. The advantage of using the recursive lattices for the thermodynamic calculations was pointed by Gujrati [53] in connection with a simple trick that allows the calculation of the free energy ω, and various densities exactly.

A. Recursion relations

1. Site labeling

The cactus has a central plaquette, which is connected to four plaquettes, each of which is connected to three other plaquettes, and so on; see Figs. 1(a) and 1(b). Following [8–10,53], the lattice sites are indexed by a level index m, which increases as we move away from the center of the cactus; see Fig. 1(a), which represents dimers (shown by thick bonds) forming a columnar phase with all dimers in the horizontal orientation. If the base site, the site closer to the cactus center of a given square, is labeled m, then the other three sites of the square (the two intermediate sites connected to the base and the peak site connected to the intermediate sites) are indexed $(m+1)$. This square is indexed as mth square and is connected to three $(m+1)$th squares. In addition, we need some way to capture the ground states that do not possess the trivial 1-cycle (isotropic) translational symmetry. The columnar ground state [Fig. 1(a)] has the apparent 2-cycle symmetry, while the staggered state [Fig. 1(b)] has a new type of symmetry which we describe by introducing another index α. It is used to distinguish the four sites of a plaquette; see Fig. 1(b), which represents the staggered phase. The central plaquette has its four sites labeled 1,2,3, and 4 in a clockwise manner. The four sites in all other plaquettes are labeled identically in a clockwise fashion, except that we suppress the labeling of the base site in each plaquette. The reason of such labeling will be clear from our further description of the calculation method.

2. Site states and partial partition functions

There are five possible states for a site on the lattice. It is either occupied by a solvent (to be denoted by s) or by a dimer endpoint with the dimer pointing along one of the four bond directions that we denote by horizontal going up, i.e., pointing away from the origin ($\mathrm{h_u}$), or down, i.e., pointing towards the origin ($\mathrm{h_d}$), and vertical going up or down ($\mathrm{v_u}, \mathrm{v_d}$). We introduce the partial partition functions (PPF) $Z_m^{(\alpha)}(i)$, given that the site (m,α) is in the state $i = \mathrm{s}, \mathrm{h_u}, \mathrm{h_d}, \mathrm{v_u}, \mathrm{v_d}$. It represents the contribution to the total partition function from the part of the tree above mth level site (m,α) in the ith state.

3. Recursion relations

We then obtain the RR's between $Z_m^{(\alpha)}(i)$ at level m and the PPF's at the higher level $(m+1)$ by considering all possibilities and the local statistical weights of the $(m+1)$th square. In the most general case, the RR's for the PPF's are given by a cubic polynomials for a square Husimi cactus:

$$Z_m^{(\alpha)}(i) = \sum w_{jkp}^{(\gamma\delta\alpha)} Z_{m+1}^{(\gamma)}(j) Z_{m+1}^{(\alpha)}(k) Z_{m+1}^{(\delta)}(l), \tag{22}$$

where j, k, and l are the states of the three sites at the level $(m+1)$ (in the clockwise direction from the base site) for each allowed configuration inside the mth level polygon and the base site is in the state i. The local statistical weight is given by $w_{jkl}^{(\gamma\alpha\delta)}$. The upper indices are $(\gamma\alpha\delta)=(412)$, (123), (234), and (341) for $\alpha=1$, 2, 3, and 4, respectively. We wish to note that we find it convenient to absorb the solvent activity η in the defionition of $Z_m^{(\alpha)}$(s). We define

$$B_m^{(\alpha)} \equiv \sum_i Z_m^{(\alpha)}(i), \tag{23}$$

in which the sum is over all states i, to introduce the ratios

$$x_{i,m}^{(\alpha)} \equiv Z_{m+1}^{(\alpha)}(i)/B_{m+1}^{(\alpha)}. \tag{24}$$

It is obvious that the ratios are always less than or equal to 1, and satisfy the sum rule

$$\sum_i x_{i,m}^{(\alpha)} = 1. \tag{25}$$

The above RR's among the partial PF's are then converted into RR's relate $x_{i,m}^{(\alpha)}$ with the ratios at the higher level $(m+1)$:

$$x_{i,m}^{(\alpha)} = P_{i,m+1}^{(\alpha)}/Q_{m+1}^{(\alpha)}, \tag{26}$$

where $P_{i,m}^{(\alpha)}$ are various polynomials given by the right-hand side of (22) in which the PPF's are replaced by the corresponding ratio given in (24) and

$$Q_m^{(\alpha)} = \sum_i P_{i,m}^{(\alpha)}. \tag{27}$$

The explicit expressions for $P_{i,m}^{(\alpha)}$ are given in the Appendix.

B. Fix-point solutions

The fix-point (FP) solution of the RR's describe the behavior in the interior of an infinite Husimi cactus. The FP solution can be obtained numerically or analytically (when possible). There are two different kinds of FP solutions. In the 1-cycle FP solution, the ratios remain the same at consecutive levels. We denote the FP values of the ratios by $\{x_i^{(\alpha)}\} \equiv \{s^{(\alpha)}, h_{\mathrm{u}}^{(\alpha)}, h_{\mathrm{d}}^{(\alpha)}, v_{\mathrm{u}}^{(\alpha)}, v_{\mathrm{d}}^{(\alpha)}\}$. We wish to emphasize that the italicized quantities $h_{\mathrm{u}}^{(\alpha)}$, etc. represent the values of the FP, and should not be confused with the states $\mathrm{h_u}$, etc. In the 2-cycle FP solution, the ratios alternate between two successive levels, which are referred to as *even* and *odd* in the following. In order to emphasize the 2-cycle nature of the solution when necessary, the ratios on even levels are denoted without prime, and on odd levels with prime. The free energy is calculated using the method originally proposed by Gujrati [53] for the 1-cycle FP and its extension given in [9] for the 2-cycle FP. The complete details are given in [54]. The FP solution that maximizes the osmotic pressure over a

temperature range represents the equilibrium state over that range. This exact solution is taken as the *approximate* theory for the square lattice. The approach allows us to describe both the ordered, i.e. the crystal (CR) phase at low temperatures and the disordered, i.e. the equilibrium liquid (EL) phase at high temperatures. In addition, an intermediate phase (IP) with intermediate orientational order [more ordered with respect to EL and less ordered with respect to CR] is discovered by the analysis and is involved in a liquid-liquid transition induced by orientational interactions; see below for a complete description. True equilibrium states are those that minimize the relevant free energy. Abandoning this minimization principle allows us to obtain metastable states by continuing various solutions [13]. The continuation of EL to lower temperatures describes the supercooled liquid (SCL), which as we show here exhibits the entropy crisis at $T=T_K$. The disordered liquid EL for the attractive case and SCL for the repulsive case undergo a transition to IP. The continuation of IP to lower temperatures also exhibits an entropy crisis of its own at a temperature $T=T'_K$ that is usually different from T_K. We study various contact densities in CR, IP and EL, and their continuation. The densities contributing to the energy of different states, upon continuation, approach their corresponding values for CR as $T\to 0$. Thus, all phases will have *identical* free energies at $T=0$ if they can exist there. This is consistent with the claim S3. This equality [8,13] ensures that each of the two metastable states obtained by continuing EL and IP will exhibit entropy crisis.

V. RESULTS

We consider the cases $\eta=0$ ($\mu\to-\infty$), and $\eta>0$, separately as we are able to obtain analytical solutions for the former case. For the case $\eta=0$, ω is related to the Helmholtz free energy $F(T)$: $F(T)=-T\omega$ [8]. For $\eta>0$, π_0 is related to the thermodynamic potential $F(T)=-\pi_0$. To cover both cases together we define the following shifted thermodynamic potential $\bar{F}$:

$$\bar{F}(T) \equiv F(T) - F(0) = -T\omega - E_0,$$

where E_0 is the energy of the perfect CR at $T=0$. The shifted potential has the property that it vanishes at $T=0$. The vanishing of entropy corresponds to the maximum in $\bar{F}(T)$.

A. Disordered phase: EL and SCL

The disordered phase is the continuation of the phase at infinite temperatures, where the correlations are minimal. This phase is described by a 1-cycle FP solution and for which the labeling α is irrelevant ($x_i^{(1)}=x_i^{(2)}=x_i^{(3)}=x_i^{(4)}\equiv x_i$).

1. Absence of solvent

The system of RR's given in the Appendix simplifies when s is set to 0 and the index α is suppressed:

$$\begin{aligned} h_d^* &= [(w_a w_p)^2 h_u^3 + 3 w_a w_p v_u^2 h_u + (1+2 w_a w_p) v_u^2 h_u + w_a w_p v_u^3 \\ &\quad + w_a h_d^2 h_u + h_d^2 v_u + w_p h_u v_d^2 + v_u v_d^2]/Q, \\ v_d^* &= [w_a w_p h_u^3 + 3 w_a w_p v_u^2 h_u + (1+2 w_a w_p) h_u^2 v_u + (w_a w_p)^2 v_u^3 \\ &\quad + h_d^2 h_u + w_p h_d^2 v_u + h_u v_d^2 + w_a v_u v_d^2]/Q, \\ v_u^* &= v_d (w_p h_u^2 + 2 v_u h_u + w_a v_u^2 + w_p^2 v_d^2)/Q, \\ h_u^* &= h_d (w_p v_u^2 + 2 v_u h_u + w_a h_u^2 + w_p^2 h_d^2)/Q, \end{aligned} \tag{28}$$

where the polynomial Q, see (27), is given by the sum of the numerators of the right-hand sides in the above equation because of the sum rule (25) for the ratios. The FP is achieved when $x_i^*\to x_i$. The adimensional free energy ω is calculated using the Gujrati trick [53], see the Appendix:

$$\omega = (1/2)\ln(Q/Q_0),$$

where

$$Q_0 = 2 v_u v_d + 2 h_u h_d.$$

We can also calculate the densities of various types of contacts. For this, we consider the single square at the origin and consider all of their possibilities that contribute to the quantities of interest. Dividing this contribution with the total PF Z_0 yields the density per site as $\phi_\lambda=\Phi_\lambda/QQ_0$, $\lambda=$p,a, where

$$\begin{aligned} \Phi_p &= w_p (2 w_a h_u^2 v_u^2 + v_d^2 h_u^2 + h_d^2 v_u^2 + 2 w_a v_u^3 h_u)/2 + w_a v_u h_u^3 \\ &\quad + w_p^2 (w_a^2 v_u^4 + w_a^2 h_u^4 + h_d^4 + v_d^4)/2, \end{aligned} \tag{29}$$

$$\begin{aligned} \Phi_a &= w_a (2 w_p v_u h_u^3 + v_d^2 v_u^2 + 2 w_p v_u^3 h_u + 2 w_p v_u^2 h_u^2 + h_d^2 h_u^2) \\ &\quad + (w_a w_p)^2 (h_u^4 + v_u^4). \end{aligned} \tag{30}$$

There is an additional symmetry in the FP solution of interest for the disordered phase. This symmetry corresponds to having

$$\begin{aligned} h_u &= v_u \equiv a, \\ h_d &= v_d \equiv b. \end{aligned} \tag{31}$$

The resulting system of FP equations

$$\begin{aligned} b &= (a^3 K_1 + a b^2 K_2)/Q, \\ a &= (b a^2 K_2 + b^3 w_p^2)/Q, \\ Q &= 2(a^3 K_1 + a b^2 K_2 + b a^2 K_2 + b^3 w_p^2), \end{aligned}$$

where

$$\begin{aligned} K_1 &= (w_a w_p)^2 + 6(w_a w_p) + 1, \\ K_2 &= w_a + w_p + 2, \end{aligned}$$

can be solved analytically making the substitution $r=b/a$:

$$r = (K_1/w_p^2)^{1/4}. \tag{32}$$

Using the sum rule $2a+2b=1$, which follows from (25), we eventually have

$$\begin{aligned} Q^{\rm dis} &= ab(K_2 + \sqrt{K_1 w_p^2}), \\ Q_0^{\rm dis} &= 4ab. \end{aligned}$$

The analytical expressions giving the free energy and the entropy of the system as functions of temperature for EL and SCL states for the system of directionality interacting dimers (no solvent) are presented below

$$\omega^{\mathrm{dis}} = \tfrac{1}{2}\ln(K_2 + \sqrt{K_1 w_{\mathrm{p}}^2}) - \ln 2,$$

$$\phi_{\mathrm{p}}^{\mathrm{dis}} = \frac{3w_{\mathrm{p}}w_{\mathrm{a}} + w_{\mathrm{p}}r^2 + 2(w_{\mathrm{p}}w_{\mathrm{a}})^2 + 2w_{\mathrm{p}}^2 r^4}{4r^2(K_2 + \sqrt{K_1 w_{\mathrm{p}}^2})}, \tag{33}$$

$$\phi_{\mathrm{a}}^{\mathrm{dis}} = \frac{3w_{\mathrm{a}}w_{\mathrm{p}} + w_{\mathrm{a}}r^2 + (w_{\mathrm{a}}w_{\mathrm{p}})^2}{2r^2(K_2 + \sqrt{K_1 w_{\mathrm{p}}^2})},$$

$$S_{\mathrm{dis}} = \omega^{\mathrm{dis}} - 2\phi_{\mathrm{p}}^{\mathrm{dis}}\ln w_{\mathrm{p}} - \phi_{\mathrm{a}}^{\mathrm{dis}}\ln w_{\mathrm{a}}.$$

At this point we refer to the famous calculations by Kasteleyn [55] and by Fisher [56] who provided the exact value for the number of dimer packings on a square lattice, $\varphi_{\mathrm{exact}} = 1.7916$ where φ is the molecular freedom per site, $\varphi = \exp(2S)$. The high-temperature limit of S_{dis} in (33) represents the number of configurations for weakly interacting dimers on Husimi cactus. Taking the limit $w_{\mathrm{a}} \to 1$ $w_{\mathrm{p}} \to 1$ we find $\varphi_{\mathrm{Husimi}} = 1.7071$. To appreciate the improvement due to the use of the Husimi cactus over the Bethe lattice we compare this with $\varphi_{\mathrm{Bethe}} = 1.6875$ obtained by Chang [57].

2. Presence of solvent

The effect of solvent is investigated by letting $\eta \neq 0$, i.e. by taking a finite $\mu < 0$ value and using the general RR's given in the Appendix. We now need to consider nearest-neighbor solvent -endpoint interactions, which we take not do depend on the dimer orientation. These are ordinary isotropic interactions with energy given by the standard exchange or excess expression: $\varepsilon = e_{0\mathrm{m}} - (e_{00} + e_{\mathrm{mm}})/2$, where $e_{0\mathrm{m}}$, e_{00}, and e_{mm} are direct solvent-monomer, solvent-solvent, and monomer-monomer interaction energies [49]. When the solvent represents voids, $e_{00} = e_{01} = 0$ and $\varepsilon = -1/2 e_{\mathrm{mm}}$. We are no longer able to find the FP solution analytically, and are forced to use numerical methods to find it.

B. Columnar ground state

The columnar order is attained by considering a negative value for ε_{p}. The order becomes perfect as $T \to 0$. From now on, in analogy with high-T_{c} superconductivity scenario proposed by Roksar and Kivelson [58], ε_{p} will be called the *resonance energy* and the dimer pairs that occupy the same square are called *resonating dimer* pairs. The axial interaction ($\varepsilon_{\mathrm{a}} < 0$) is not necessary although it would enhance the formation of the ordered state. In addition to the disordered equilibrium liquid EL discussed above and that is stable at high temperatures, our solution captures two ordered phases: the columnar state crystal (CR), which is the equilibrium state at low temperatures, and a phase with an intermediate order (IP), which is the equilibrium state at intermediate temperatures before EL becomes the equilibrium state.

1. Absence of solvent

At first, we study the pure dimer system with $\eta = 0$ ($\mu \to -\infty$). Three phases are distinguished by the symmetries of their FP structures. The EL solution was already described in the previous section, where it was found that $h \equiv h_{\mathrm{u}} + h_{\mathrm{d}} = v \equiv v_{\mathrm{u}} + v_{\mathrm{d}} = a + b = 1/2$. Therefore, the numbers of vertical and horizontal dimers are the same. The perfect columnar CR ($T = 0$) on the cactus has each occupied square surrounded by empty squares, and vice versa—consider the checker-board version of the sublattice structure for squares in Fig. 1(b). This property is captured by applying a 2-cycle scheme when the FP solutions for even and odd lattice sites are different. We take the convention that even (odd) squares on the Husimi cactus have even (odd) base sites. In the case when the dimers in the perfect CR occupy even squares and are oriented in the horizontal direction (horizontally resonating dimers), we have $h_{\mathrm{u}} = 1$, $v_{\mathrm{u}} = 0$, $h'_{\mathrm{d}} = 1$, $v'_{\mathrm{d}} = 0$. The perfect CR with dimers resonating vertically ($v_{\mathrm{u}} = 1, h_{\mathrm{u}} = 0, v'_{\mathrm{d}} = 1, h'_{\mathrm{d}} = 0$) or resonating dimers occupying odd squares are disjoint from the above horizontally resonating CR phase and does not have to be considered separately. As the temperature is raised, CR begins to distort such that h_{u}, and h'_{d} decrease and v_{u}, and v'_{d} increase. On the other hand, IP is given by a solution which satisfies $h_{\mathrm{u}} = v_{\mathrm{u}} = h'_{\mathrm{d}} = v'_{\mathrm{d}} = 1/2$ and which is *independent* of the temperature. The 2-cycle structure of the solution suggests that dimers continue to resonate locally occupying even squares, but resonating pairs on average have no preference whether to orient horizontally or vertically. Therefore, we can say that the IP is characterized by the positional order but no orientational order, and resemble more like a *plastic crystal*. Another analogy comes from quantum dimer problem, where the so- called plaquette phase with similar properties is observed [59].

The perfect CR that has $T\omega^{\mathrm{ord}} = -\varepsilon_{\mathrm{p}}$, $S_{\mathrm{ord}} = 0$, $\phi_{\mathrm{p}}^{\mathrm{ord}} = \phi_{\mathrm{a}}^{\mathrm{ord}} = 1/2$ is thermodynamically stable at temperatures close to zero as expected. It is depicted in Fig. 2 by filled diamonds. In the following we assume that all dimers are resonating horizontally. As the CR heats up, resonating dimer pairs begin to resonate in the vertical direction maintaining their positions within even squares with the result that S_{ord} increases, and $\phi_{\mathrm{p}}^{\mathrm{ord}}$ and $\phi_{\mathrm{a}}^{\mathrm{ord}}$ decrease. At some point, CR undergoes a continuous transition and a new state IP appears (filled triangles); the transition point is shown in Fig. 2 at $T_{\mathrm{IP}} \cong 1.74$. In IP, the densities of resonating dimers in the two directions remain *equal* to each other. The density of resonating dimers $\phi_{\mathrm{p,res}}^{\mathrm{IP}} = 1/4$, resonating within either odd or even squares only, remains independent of the temperature, while $\phi_{\mathrm{p}}^{\mathrm{IP}}$ continues to decrease slowly. We also have ($K_1 = 1 + 6w_p + w_p^2$)

$$\phi_{\mathrm{a}}^{\mathrm{IP}} = (3w_{\mathrm{p}} + w_{\mathrm{p}}^2)/2K_1, \quad \phi_{\mathrm{p}}^{\mathrm{IP}} = 1/4 + \phi_{\mathrm{a}}^{\mathrm{IP}}/2,$$

$$\omega^{\mathrm{IP}} = (1/2)\ln(K_1) - \ln\sqrt{2}.$$

Figure 2 shows the equilibrium states by filled symbols, EL-metastable extension SCL at lower temperatures by the empty circles, and IP-metastable extensions at higher and lower temperatures by empty triangles. The equilibrium status is resolved by comparing the free energy $\bar{F}$ for all solutions obtained at a given temperature as shown in Fig. 2. We

also present configurational entropy S and the specific heat curves C and the contact densities ϕ_a and ϕ_p in the same figure. Note that the configurational entropy becomes zero at the point where $\bar{F}(T)$ is maximum. Below the maximum, the entropy becomes negative and, therefore, this portion of the extension cannot represent any realizable state. The extensions are shown by the smaller symbols. Thus, the maximum in $\bar{F}(T)$ locates the Kauzmann or ideal glass temperature. We also note that both SCL and the supercooled IP states exhibit the entropy crisis. According to ideas traced back to times of entropy crisis discovery [1,16], a metastable curve must be *terminated* at its Kauzmann point where the system undergoes an *ideal glass* transition, the ideal glass being a frozen and unique disordered structure. Note that the transition is not dictated by the statistical mechanical treatment, but by an additional requirement that the configurational entropy be non-negative; see S4 above. The emergence of an ideal glass cannot be verified experimentally due to tremendous slowing down below the experimentally observed glass transition. We emphasize here that the above entropy crisis has been demonstrated for the first time in an explicit calculation for a model of molecular liquid.

The EL undergoes a first-order transition to IP at the melting temperature, $T_M \cong 3.58$ in Fig. 2. The continuation of EL below T_M gives rise to SCL, whose entropy vanishes near $T_K \cong 0.64$. Similarly, the continuation of IP below T_c describes its metastable state whose entropy also vanishes near $T'_K \cong 0.44$, thus giving rise to another entropy crisis. Our exact calculation also shows that the contact densities of both metastable states approach the values for the ideal crystal as $T \to 0$, namely $\phi_a^\kappa, \phi_p^\kappa \to 1/2$, where κ=dis, IP, and CR. Equality of ϕ_p^κ is consistent with the energy equality at $T=0$; see S3 above. The equality of ϕ_a^κ is due to the fact that it is determined uniquely by ϕ_p^κ at $T=0$. The entropies of the metastable branches approach negative values at $T=0$: $S_{IP} \to -\ln\sqrt{2}$, and $S_{dis} \to -\ln 2$.

The differences between the three phases can be summarized as follows. Let $h \equiv h_u + h_d$, = and $v \equiv v_u + v_d$ at each level, whether even or odd. (For odd levels, we have primed quantities.) The calculation shows the following.

(1) EL has the 1-cycle structure and has $h=v$ at each level.

(2) IP has the 2-cycle structure but still has $h=v$ at each level.

(3) CR has the 2-cycle structure but does not satisfy $h=v$ at each level.

2. Presence of solvent: Localization

The presence of solvent eventually turns the melting transition second-order. Figure 3 includes the curves for a typical solvent density dependence, and the ratio of the density of solvent-solvent contacts to the solvent density,

$$D_0 \equiv \phi_{00}/\phi_0.$$

The ratio $D_0 \equiv N_{00}/N_0$ representing the number of solvent-solvent contacts per solvent is a measure of solvent localization. This quantity helps us in understanding the clustering of solvents (see [60] for quantum dimer model analogy), and

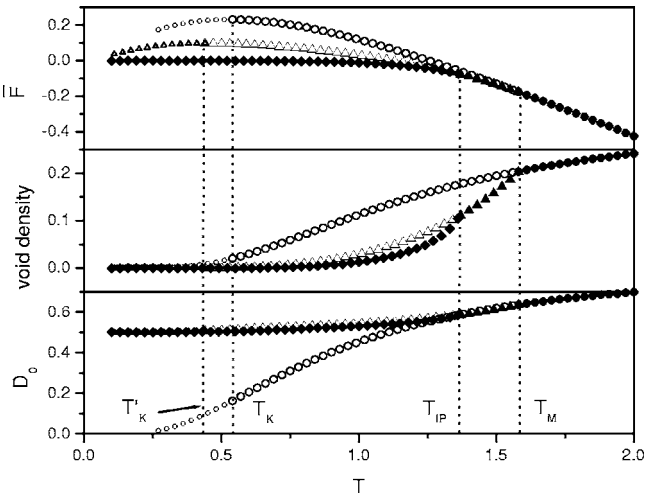

FIG. 3. Solvent density effects ($\varepsilon_p=-1, \varepsilon_a=0, \varepsilon=0.1, \mu=-0.1$).

can be used to answer the question: Will solvent pairs initially introduced by taking out some dimers break upon or coalesce after establishing equilibration? If the solvent particles were randomly distributed, then $\phi_{00}=2\phi_0^2$, so that $D_0=2\phi_0$. If the solvent particles were paired as two nearest-neighbor solvent particles (dimerized solvent) so as to replace a dimer, then $\phi_{00}=\phi_0/2$, and $D_0=1/2$. If the solvent particles appear as a cluster of four to replace two dimers inside a square, then $D_0=1$, and so on. Thus, ϕ_{00}/ϕ_0 provides us with the information about the nature of their distribution. We expect the random distribution at very high temperatures. From Fig. 3, we see that D_0 is slightly larger than ϕ_0 at higher temperatures, implying that the solvent distribution is still highly correlated. At low temperatures, we find that $D_0^{CR}=D_0^{IP}=1/2$, indicating that solvents appear in the form of a dimerized solvent to replace a single dimer. In contrast, D_0^{SCL} approaches zero, implying that the solvents are not dimerized in it. This is an interesting observation in view of the fact that all have vanishingly small solvent density near absolute zero. At higher temperatures, ϕ_0^{SCL} is much higher than ϕ_0^{CR} and ϕ_0^{IP}.

3. Presence of axial interactions

Introducing attractive axial interactions makes CR to be stable at higher temperatures, thus destroying IP. The higher the strength of the attractive axial interactions, the larger $|\varepsilon_a|$, the higher T_c moves. Large enough $|\varepsilon_a|$ destroys the stable portion of IP resulting in second-order liquid-liquid transition to occur in SCL region, see Fig. 4. Once ε and μ are kept constant, increasing $|\varepsilon_p|$ results in higher melting and Kauzmann temperatures, and larger solvent (free volume) densities.

C. Staggered ground state

1. Absence of solvent

The staggered ground state with all dimers aligned in one direction, taken to be horizontal in Fig. 1(b), is achieved only

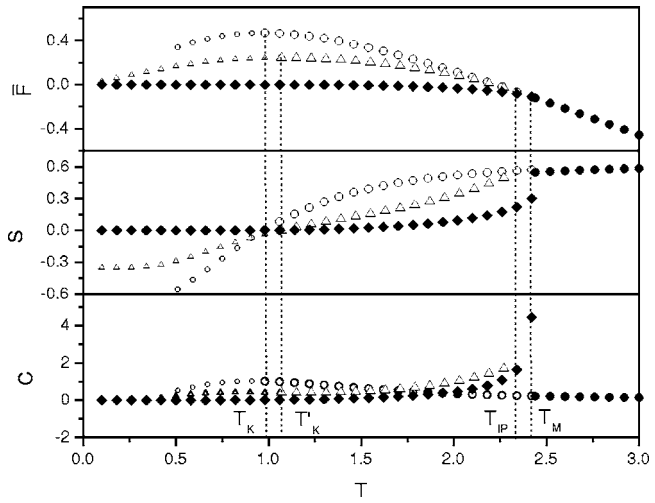

FIG. 4. The same as Fig. 2, but for $\varepsilon_p=-0.2$, $\varepsilon_a=-1.5$, $\varepsilon=0.1$, and $\mu=-0.1$ We show that increasing the strength of the attractive axial interaction causes IP to appear in the SCL region.

when, in addition to the repulsive parallel-dimer interaction, an attractive axial interaction is introduced. Moreover, the staggered state requires a different description than the one used to describe the columnar phase studied above. The two intermediate sites in a given square on the cactus are in different states, but the upper and the base lattice sites are in the same state. In order to capture this particular property of the ground state, we need to distinguish the four sites by the index $\alpha=1$, 2, 3 and 4. As in the previous case, three types of FP solutions of different symmetries are obtained: the disordered liquid EL discussed earlier, the crystal (CR), and the intermediate phase (IP). The situation is depicted in the Figs. 5–7. The filled circles and diamonds represent the equilibrium states EL and CR, respectively, with a discontinuous transition between them at the melting point T_M. We also show their metastable extensions depicted by empty circles (SCL) and empty diamonds (superheated CR). A liquid-liquid continuous transition occurs at T_{IP} between SCL and

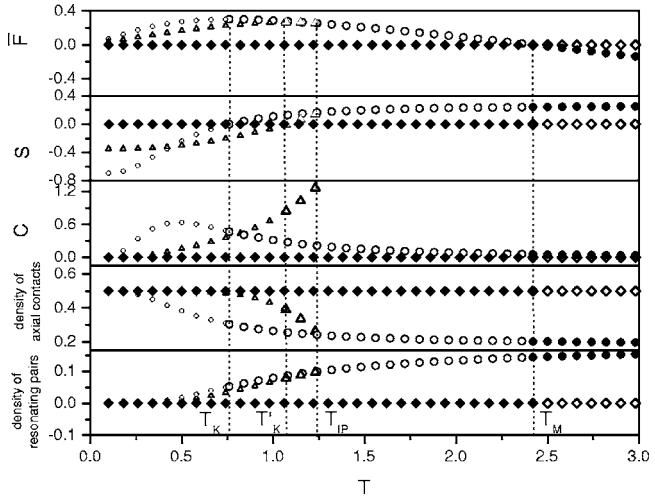

FIG. 5. The same as Fig. 2, but for $\varepsilon_p=1$, $\varepsilon_a=-1$, and $\eta=0$. We find the liquid-liquid transition at $T_{IP}<T_M$.

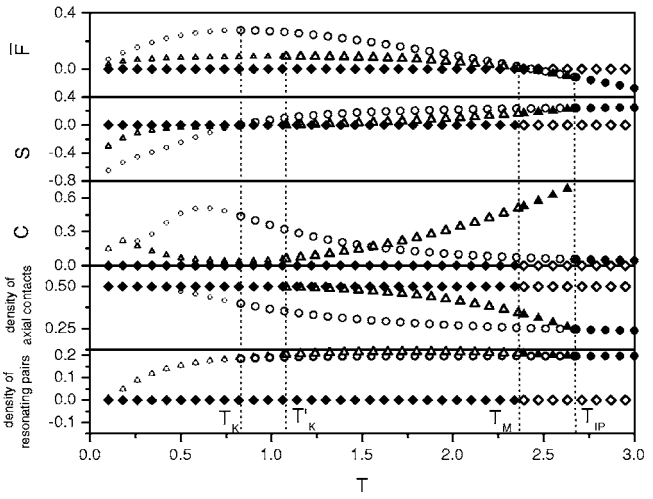

FIG. 6. The same as Fig. 2, but for $\varepsilon_p=0.2$, $\varepsilon_a=-2$, and $\eta=0$. We find the liquid-liquid transition at $T_{IP}>T_M$.

IP. The later is shown by triangles, which originates at T_{IP} and continues all the way down to absolute zero, just like SCL. It is clear from Fig. 5 that both SCL and IP exhibit the entropy crisis at T_K and T'_K, respectively. We show their extensions below their respective Kauzmann temperatures by smaller empty symbols.

The equilibrium state EL at high temperatures has been described above where the index α was omitted. Our numerical solution for the system of 1-cycle RR's that result when α is taken into account predicts the same free energy and densities as given by (33). However the new solutions have a slightly different symmetry $(x_i^{(1)}=x_i^{(3)}),(x_i^{(2)}=x_i^{(4)})$ whereas the earlier EL solution requires the symmetry $(x_i^{(1)}=x_i^{(3)})=(x_i^{(2)}=x_i^{(4)})$. (The latter symmetry can be obtained by an appropriate choice of the initial guesses for the RR's given in the Appendix.) In addition, the solution also has the following symmetry: $h^{(\alpha)}\equiv h_u^{(\alpha)}+h_d^{(\alpha)}=v^{(\alpha)}\equiv v_u^{(\alpha)}+v_d^{(\alpha)}$. The symmetry of IP is somewhat similar to that of EL. It is also obtained in a 1-cycle scheme and has the partial symmetry $(x_i^{(1)}=x_i^{(3)}),(x_i^{(2)}=x_i^{(4)})$, but $h^{(\alpha)}\neq v^{(\alpha)}$. The four possible 1

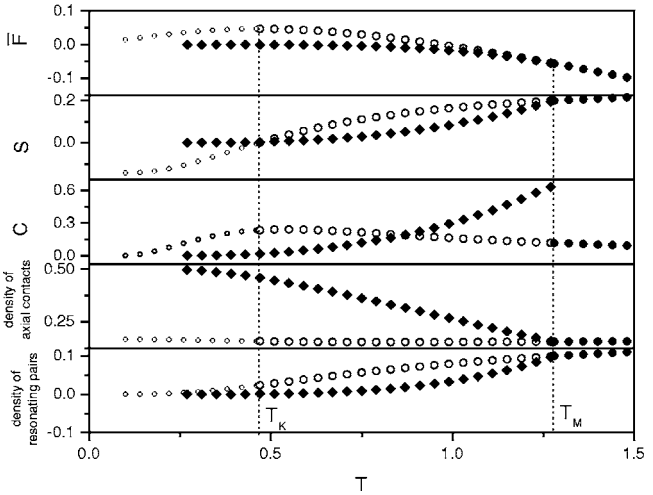

FIG. 7. The same as Fig. 2, but for $\varepsilon_p=1$, $\varepsilon_a\to 0$, and $\eta=0$.

-cycle solutions representing four disconnected CR states at $T=0$ are:

$$\begin{aligned} &1.\ h_{\mathrm{u}}^{(1)}=h_{\mathrm{d}}^{(2)}=h_{\mathrm{d}}^{(3)}=h_{\mathrm{u}}^{(4)}=1.\\ &2.\ h_{\mathrm{d}}^{(1)}=h_{\mathrm{u}}^{(2)}=h_{\mathrm{u}}^{(3)}=h_{\mathrm{d}}^{(4)}=1.\\ &3.\ v_{\mathrm{u}}^{(1)}=v_{\mathrm{u}}^{(2)}=v_{\mathrm{d}}^{(3)}=v_{\mathrm{d}}^{(4)}=1.\\ &4.\ v_{\mathrm{d}}^{(1)}=v_{\mathrm{d}}^{(2)}=v_{\mathrm{u}}^{(3)}=v_{\mathrm{u}}^{(4)}=1. \end{aligned} \tag{34}$$

Only one of the above four CR states will occur due to symmetry breaking. Thus, the other three FP solutions do not need to be considered.

The staggered phase is an example of a frozen state, which does not allow creating any local imperfections when voids or solvents are forbidden. Once trapped in it at low T, the system remains frozen in a single microstate as the temperature is elevated further. This is indicated by the temperature-independent osmotic pressure for CR. Consequently, the CR entropy $S_{\mathrm{ord}}=0$. In addition, $\phi_{\mathrm{a}}^{\mathrm{ord}}=1/2$ and $\phi_{\mathrm{p}}^{\mathrm{ord}}=0$ remain constant. As expected, CR is the equilibrium state at low temperatures, while EL is the equilibrium state at high temperatures. The melting transition between these two states takes place at $T_{\mathrm{M}}\cong 2.42$ (Fig. 5) where densities change discontinuously. Both CR and EL have their extensions into the metastable region shown by means of empty symbols. The EL extension below T_{M} yields SCL. Another metastable liquid phase IP is found in the SCL region where it meets continuously with SCL via a second-order liquid-liquid transition at $T_{\mathrm{IP}}\cong 1.24$. The new phase IP has much higher ϕ_{a} and lower ϕ_{p} relative to SCL so that the dimers are preferentially oriented in one direction in IP. The specific heat curves for SCL and IP show relatively large discontinuity at T_{IP}.

Both SCL and IP exhibit their own entropy crises at different temperatures, $T_{\mathrm{K}}\cong 0.76$ and $T'_{\mathrm{K}}\cong 1.07$ respectively. Although they are not absolutely stable compared to CR, the free energy ω^{IP} of the IP is higher than that of SCL. The calculation predicts negative configurational entropies for the extensions of SCL and IP below their Kauzmann temperatures represented by smaller empty symbols in Fig. 5. The density values for the extensions of EL and IP reach the crystalline values at $T=0$ so that SCL, IP, and CR have the same energy $E_0=\varepsilon_{\mathrm{a}}/2$; see S3 above. Thus, our exact calculations confirms the theorem of identical energies of all possible stationary states proven in [13]. We also find that the entropies of SCL and IP are extrapolated to $-\ln 2$ and $-\ln\sqrt{2}$ respectively at $T=0$, so that $TS\to 0$ as $T\to 0$, a condition for the identical energy theorem.

Changing ε_{p} affects T_{M} much stronger than T_{IP}, viz. T_{M} decreases with reduction of ε_{p}. Figure 6 demonstrates the situation when $T_{\mathrm{IP}}\cong 3.0$ is moved above $T_{\mathrm{M}}\cong 2.39$. We also have $T_{\mathrm{K}}\cong 0.83$ and $T'_{\mathrm{K}}\cong 1.08$.

The liquid-liquid transition temperature moves towards the melting temperature as the strength $|\varepsilon_{\mathrm{a}}|$ of the attractive axial interactions increases. At the same time, the melting temperature rises with $|\varepsilon_{\mathrm{a}}|$. Reducing axial attraction eventually makes IP to appear below T_{K} only. Thus, IP is induced by axial interactions. In the limit when $|\varepsilon_{\mathrm{a}}|\to 0$, IP disappears from the phase diagram completely, see Fig. 7. The ground state is a highly degenerate state represented by configurations with no dimer pairs occupying the same lattice square, which we call a staggered ladder phase. The actual configuration that is captured numerically depends on the initial guess (boundary condition) in the RR's and the structure of RR's. Figure 7 shows that obtained crystalline state has $\phi_{\mathrm{a}}^{\mathrm{ord}}=1/2$ at $T=0$, while $\phi_{\mathrm{a}}^{\mathrm{SCL}}$ approaches to $1/6$ at $T=0$. The latter value is consistent with the analytical expression (33). We conclude that the ideal glass state achieved at T_{K} is a unique disordered state even if the ordered ground state is highly degenerate.

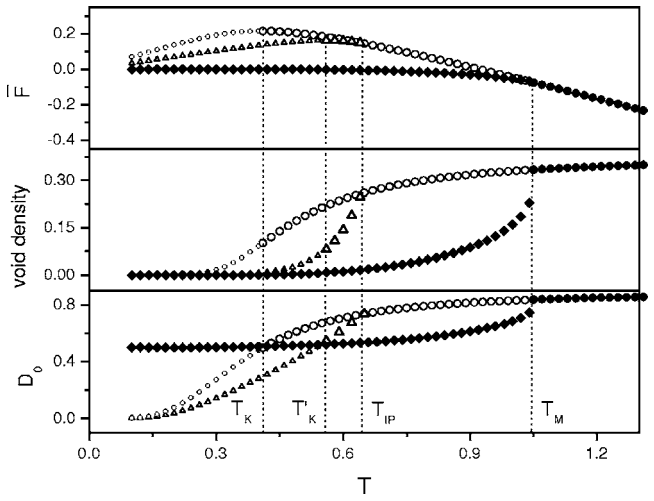

FIG. 8. Solvent density effects ($\varepsilon_{\mathrm{p}}=1$, $\varepsilon_{\mathrm{a}}=-1$, $\varepsilon=0.1$, and $\mu=-0.1$).

The differences between the three phases can be summarized as below. The calculation shows the following.

(1) EL has the property $h=v$ at each level for each α, and individual $x_i^{(1)}=x_i^{(3)}$, and $x_i^{(2)}=x_i^{(4)}$.

(2) IP does not have the property $h=v$ at each level for each α, but still has $x_i^{(1)}=x_i^{(3)}$, and $x_i^{(2)}=x_i^{(4)}$.

(3) CR has neither of the properties of EL.

2. Presence of solvent

The crystalline state is no longer frozen when the solvent is introduced. As we increase μ and decrease ε, the discontinuous in densities at T_{M} become smaller and smaller. Eventually melting transforms into a second-order transition. The presence of the solvent makes T_{M} go down; The larger μ and the smaller ε are, the smaller T_{M} becomes. Figure 8 shows the solvent density ϕ_0. Compared to the case of $\varepsilon_{\mathrm{p}}<0$, the values of ϕ_0 at the Kauzmann temperatures are much larger. The solvent density in SCL is larger than in IP and the same holds for the ratio D_0.

VI. DISCUSSION AND CONCLUSIONS

We have argued that the configurational entropy is the central concept and has to be defined properly and carefully if we have any chance of success in explaining the experi-

mentally observed glass transition in supercooled viscous liquids. We have followed the conventional definition of the configurational entropy, which is obtained by considering the configurational degrees of freedom and is obtained by subtracting the entropy $S_{\rm KE}(T)$ due to the translational degrees of freedom from the total entropy. It is this configurational entropy that is used to define the configurational partition function. This definition is compared with the other definitions of configurational entropy used by experimentalists and in other theories. We show that the many other definitions are operational in spirit to estimate the configurational entropy since the latter is not experimentally accessible, at least at present by any known technique.

We should clarify the notion of the configurational PF, which emerges as a factor in the product in (5), for the case of dimers that we consider here for explicit calculation. The fixed length of the dimer means that it has no vibration as would occur in a diatomic molecule. Hence, it should be treated as a rigid particle with only five degrees of freedom: three center-of-mass translational and two rotational. Thus, the factor $(2\pi\hbar)^{3N}$ in (6) should be replaced by $(2\pi\hbar)^{5N_{\rm d}/2}$, $N_{\rm d}$ being the number of dimers. Furthermore, $Z_{\rm KE}(T)$ will only contain the translational and rotational kinetic energies associated with the five degrees of freedom; there are no spatial coordinates in it. Accordingly, $Z_{\rm T}(T)$ still has a factorization property, which has been used here in this work.

The current definition of the configurational entropy has the virtue that it is non-negative for realizable states in Nature. This is not true of some of the other definitions of the configurational entropy that are common in the field. (The entropy due to inherent structures [37] and the complexity [46] remain non-negative, and do not suffer from this problem.) Thus, we warn the reader to carefully appreciate this important distinction between our definition and other available definition. In particular, Kauzmann [1] had considered the excess entropy $S_{\rm ex}(T)$ as the quantity whose rapid drop upon extrapolation to negative values was interpreted by him as representing the entropy crisis that is avoided by the impending glass transition. However, there is no thermodynamic reason why $S_{\rm ex}(T)$ could not be negative [12]. We avoid this problem by considering $S(T)$, which must remain non-negative. We, thus, modify the original suggestion of Kauzmann, and adopt the view that observing $S_{\rm SCL}<0$ under extrapolation of experimental $S_{\rm SCL}$ implies a genuine entropy crisis in that such extrapolated states cannot exist. Any state to be observed in Nature must, as a prerequisite, have a non-negative entropy. This principle must be obeyed by any observed state in Nature, regardless of whether the state is an equilibrium state, metastable state of partial equilibrium, or a stationary metastable state. We have shown that while it is possible in theoretical investigations to probe the stationary limit of SCL or other metastable states and be able to investigate the ideal glass transition, which is invoked to avoid the configurational entropy crisis ($S_{\rm SCL}<0$), it is impossible to establish the existence of the ideal glass transition without the help of extrapolation in experiments or numerical simulation, since they only deal with states that exist in Nature. Consequently, they will only access states for which the configurational entropy must strictly be non-negative and will never access the region of negative entropy except by extrapolation.

Since the value of the configurational entropy is crucial in locating the Kauzmann temperature, we discuss how to define the entropy properly ($S\geqslant 0$) by discretizing the real and momentum spaces. This procedure ensures $S\geqslant 0$. We then argue that since the translational degrees of freedom are decoupled from the configurational degrees of freedom, we need to ensure the non-negativity of each of the entropy from the two decoupled degrees of freedom. Since the entropy due to the kinetic energy is always non-negative, we need to only verify whether the configurational entropy is non-negative so that the entropy crisis would not occur for realizable states.

We have adopted the view, following Penrose and Lebowitz [47], that the continuation of the disordered state (EL) free energy below the melting temperature represents the stationary limit of the supercooled liquid as long as the entropy remains non-negative. We have considered two different PF's $Z_{\rm dis}(T)$ and $\hat{Z}_{\rm dis}(T)$. While $\hat{Z}_{\rm dis}(T)$ is the right PF to obtain the free energy continuation of EL, the method of calculation can only evaluate $Z_{\rm dis}(T)$. Thus, the ideal glass state has to be introduced by hand, as we do here.

One of the major aims of the work was to establish the existence of the entropy crisis in metastable molecular fluids. We have developed a simple model of molecular fluids composed of dimers. The model is defined on a lattice so that it only contains configurational entropy and contains directional and direction-independent interactions. One of the former interactions is the interaction between the end-points of the dimers, which is either attractive or repulsive, and is used to broadly classify the molecular liquid into attractive and repulsive cases. This is because the CR-symmetries in the two cases are very different, as shown in Fig. 1.

The model is solved exactly on a special kind of recursive lattices, commonly known as the site-sharing Husimi cactus. The cactus is an approximation of a square lattice and shares with it the coordination number and the smallest loop size. The method of solution uses recursive technique, which is standard by now. What distinguishes the present analysis with most other similar investigations is that the ordered phase (CR and IP) descriptions require identifying novel FP structures with appropriate symmetries, which are very different from the symmetry of the FP solution describing the disordered phase (EL and its metastable extension SCL). This also requires us to calculate the osmotic pressure ($\eta>0$) or the free energy ($\eta=0$) appropriately.

Because of the directional interactions, we also obtain an intermediate phase IP, which may or may not be an equilibrium state depending on the directional interactions. In the attractive case, IP is an equilibrium state, but its extension at low temperatures is a metastable state with respect to CR. However, for $\varepsilon_{\rm p}>0$, it is a metastable state in Fig. 4 and an equilibrium state in Fig. 5. In both cases, its extension at low temperatures is a metastable state with respect to CR. Both EL and IP have their extensions that exhibit their own entropy crisis. The fact that EL's metastable extension SCL exhibits an entropy crisis is not a surprise on its own, since this is what we intended to demonstrate, it came as a surprise that the metastable extension of IP (which itself may be a

metastable state with respect to CR, but an "equilibrium state" with respect to SCL) also exhibited a Kauzmann temperature of its own. This is consistent with the rigorous analysis of Gujrati [13], which demonstrates the existence of an entropy crisis in a state which is a metastable extension with respect to CR. The argument is applicable to any number of metastable extensions, as long as these extensions are of stationary nature.

The model is rich enough due to its complex energetics that we also find liquid-liquid transition in the model. The transition is driven by the directional interactions in the model. The distributions of solvent particles in the metastable states are very different from that in CR. This is seen clearly from the behavior of D_0.

The analysis of the present work also confirms the equal energy principle S3 at $T=0$ for all states that can be continued to $T=0$; here, we carry out the continuation without any regard to the principle of reality ($S \geqslant 0$). This is important as it immediately implies that there must be a positive ideal glass (i.e., a Kauzmann) temperature. We further note that $TS(T) \to 0$ for all of the states [13].

Because of the equal energy observation, the question that naturally arises is whether all the states at absolute zero represent the same state. The answer is negative in general, as we demonstrate now. It is clear that all densities that determine the energy must be the same in all states, since the equal energy principle is obeyed no matter what the values of the interaction energy parameters. However, there are other geometrical and topological quantities in the system that do not affect the energy. These quantities have no reason to be the same in all states at $T=0$. We have considered the repulsive case in which we let $\varepsilon_a=0$, so that ϕ_a does not affect the energy of the system; see Fig. 8. We find that $\phi_a^{CR}=1/2$, while $\phi_a^{SCL}=1/6$, so that it does not have the same value in all states at $T=0$. Thus, the states at absolute zero are different despite having the same energy.

In conjunction with the earlier results demonstrating the existence of a positive ideal glass transition (Kauzmann) temperature for long polymers, the present work fills the gap by showing that even molecular viscous fluids also have a positive ideal glass transition temperature. We thus conclude that the stationary metastable state must always exhibit a positive ideal glass transition temperature below which the configurational entropy will become negative no matter what the molecular size is, if we insist on extrapolation. Since a negative entropy violates the principle of reality, we are forced to conclude that a new state, the ideal glass state, must be brought into the picture to replace the extrapolated state below the ideal glass transition temperature. This is, again, in conformity with S4.

Thus, we finally conclude that every (stationary) metastable state must experience an entropy crisis at a nonnegative ideal glass transition temperature, no matter what the size of the molecules is. The solvent density, which can also be treated as free volume, does not play a determining role, except when it becomes too large to destroy the entropy crisis by bringing down the ideal glass transition temperature to absolute zero. Our analysis says nothing about systems that have no ordered state for which, therefore, stationary metastability is not an issue.

ACKNOWLEDGMENTS

We would like to thank Andrea Corsi for many fruitful discussions.

APPENDIX

1. RR's in general form

We give the set of RR's being used to capture the staggered phase. At first, we calculate the polynomials $P_i^{(\alpha)}$ that are given by

$$\begin{aligned}P_s^{(1)} = {} & \eta w^2(w_a w_p h_u^{(4)} h_u^{(1)} h_u^{(2)} + h_u^{(4)} v_u^{(1)} h_u^{(2)} + w_p v_u^{(4)} v_u^{(1)} h_u^{(2)} + w_p v_u^{(4)} h_u^{(1)} h_u^{(2)} + w_a h_u^{(4)} h_u^{(1)} v_u^{(2)} + w_a h_u^{(4)} v_u^{(1)} v_u^{(2)} + w_a w_p v_u^{(4)} v_u^{(1)} v_u^{(2)} \\ & + v_u^{(4)} h_u^{(1)} v_u^{(2)} + h_d^{(4)} h_d^{(1)} h_u^{(2)} + h_d^{(4)} h_d^{(1)} v_u^{(2)} + h_u^{(4)} v_d^{(1)} v_d^{(2)} + v_u^{(4)} v_d^{(1)} v_d^{(2)} + w_p s^{(4)} h_u^{(1)} h_u^{(2)} + s^{(4)} v_u^{(1)} h_u^{(2)} + s^{(4)} h_u^{(1)} v_u^{(2)} + w_a s^{(4)} v_u^{(1)} v_u^{(2)} \\ & + w^2 h_u^{(4)} s^{(1)} h_u^{(2)} + w^2 v_u^{(4)} s^{(1)} h_u^{(2)} + w^2 h_u^{(4)} s^{(1)} v_u^{(2)} + w^2 v_u^{(4)} s^{(1)} v_u^{(2)} + h_u^{(4)} v_u^{(1)} s^{(2)} + w_a h_u^{(4)} h_u^{(1)} s^{(2)} + w_p v_u^{(4)} v_u^{(1)} s^{(2)} + v_u^{(4)} h_u^{(1)} s^{(2)} \\ & + h_u^{(4)} s^{(1)} s^{(2)} + v_u^{(4)} s^{(1)} s^{(2)} + s^{(4)} v_u^{(1)} s^{(2)} + s^{(4)} h_u^{(1)} s^{(2)} + s^{(4)} s^{(1)} h_u^{(2)} + s^{(4)} s^{(1)} v_u^{(2)} + h_d^{(4)} h_d^{(1)} s^{(2)} + s^{(4)} v_d^{(1)} v_d^{(2)}) + \eta s^{(4)} s^{(1)} s^{(2)}, \end{aligned} \tag{A1}$$

$$\begin{aligned}P_{h_d}^{(1)} = {} & w_a^2 w_p^2 h_u^{(4)} h_u^{(1)} h_u^{(2)} + w_a w_p h_u^{(4)} v_u^{(1)} h_u^{(2)} + w_a w_p v_u^{(4)} v_u^{(1)} h_u^{(2)} + w_a w_p v_u^{(4)} h_u^{(1)} h_u^{(2)} + w_a w_p h_u^{(4)} h_u^{(1)} v_u^{(2)} + w_a w_p h_u^{(4)} v_u^{(1)} v_u^{(2)} \\ & + w_a w_p v_u^{(4)} v_u^{(1)} v_u^{(2)} + v_u^{(4)} h_u^{(1)} v_u^{(2)} + w_a h_d^{(4)} h_d^{(1)} h_u^{(2)} + h_d^{(4)} h_d^{(1)} v_u^{(2)} + w_p h_u^{(4)} v_d^{(1)} v_d^{(2)} + v_u^{(4)} v_d^{(1)} v_d^{(2)} + w^2 w_a w_p s^{(4)} h_u^{(1)} h_u^{(2)} \\ & + w_a s^{(4)} v_u^{(1)} h_u^{(2)} + s^{(4)} h_u^{(1)} v_u^{(2)} + w_a s^{(4)} v_u^{(1)} v_u^{(2)} + w_a w_p h_u^{(4)} s^{(1)} h_u^{(2)} + w_a v_u^{(4)} s^{(1)} h_u^{(2)} + w_p h_u^{(4)} s^{(1)} v_u^{(2)} + v_u^{(4)} s^{(1)} v_u^{(2)} + w_p h_u^{(4)} v_u^{(1)} s^{(2)} \\ & + w_a w_p h_u^{(4)} h_u^{(1)} s^{(2)} + w_p v_u^{(4)} v_u^{(1)} s^{(2)} + v_u^{(4)} h_u^{(1)} s^{(2)} + w_a s^{(4)} s^{(1)} h_u^{(2)} + s^{(4)} s^{(1)} v_u^{(2)} + h_d^{(4)} h_d^{(1)} s^{(2)} + s^{(4)} v_d^{(1)} v_d^{(2)} + s^{(4)} s^{(1)} s^{(2)}, \end{aligned} \tag{A2}$$

$$\begin{aligned}P_{v_d}^{(1)} = {} & w_a w_p h_u^{(4)} h_u^{(1)} h_u^{(2)} + h_u^{(4)} v_u^{(1)} h_u^{(2)} + w_a w_p v_u^{(4)} v_u^{(1)} h_u^{(2)} + w_a w_p v_u^{(4)} h_u^{(1)} h_u^{(2)} + w_a w_p h_u^{(4)} h_u^{(1)} v_u^{(2)} + w_a w_p h_u^{(4)} v_u^{(1)} v_u^{(2)} + w_a^2 w_p^2 v_u^{(4)} v_u^{(1)} v_u^{(2)} \\ & + w_a w_p v_u^{(4)} h_u^{(1)} v_u^{(2)} + h_d^{(4)} h_d^{(1)} h_u^{(2)} + w_p h_d^{(4)} h_d^{(1)} v_u^{(2)} + h_u^{(4)} v_d^{(1)} v_d^{(2)} + w_a v_u^{(4)} v_d^{(1)} v_d^{(2)} + w^2 w_p s^{(4)} h_u^{(1)} h_u^{(2)} + s^{(4)} v_u^{(1)} h_u^{(2)} + w_p s^{(4)} h_u^{(1)} v_u^{(2)} \\ & + w_a w_p s^{(4)} v_u^{(1)} v_u^{(2)} + h_u^{(4)} s^{(1)} h_u^{(2)} + w_a v_u^{(4)} s^{(1)} h_u^{(2)} + w_p h_u^{(4)} s^{(1)} v_u^{(2)} + w_a w_p v_u^{(4)} s^{(1)} v_u^{(2)} + h_u^{(4)} v_u^{(1)} s^{(2)} + w_a h_u^{(4)} h_u^{(1)} s^{(2)} \\ & + w_p w_a v_u^{(4)} v_u^{(1)} s^{(2)} + w_a v_u^{(4)} h_u^{(1)} s^{(2)} + h_u^{(4)} s^{(1)} s^{(2)} + w_a v_u^{(4)} s^{(1)} s^{(2)} + w^2 s^{(4)} v_u^{(1)} s^{(2)} + w^2 s^{(4)} h_u^{(1)} s^{(2)} + s^{(4)} s^{(1)} h_u^{(2)} + w_p s^{(4)} s^{(1)} v_u^{(2)} \\ & + h_d^{(4)} h_d^{(1)} s^{(2)} + s^{(4)} v_d^{(1)} v_d^{(2)} + s^{(4)} s^{(1)} s^{(2)}, \end{aligned} \tag{A3}$$

$$P^{(1)}_{\mathrm{v_u}} = w_{\mathrm{p}} v^{(4)}_{\mathrm{d}} h^{(1)}_{\mathrm{u}} h^{(2)}_{\mathrm{u}} + v^{(4)}_{\mathrm{d}} h^{(1)}_{\mathrm{u}} v^{(2)}_{\mathrm{u}} + v^{(4)}_{\mathrm{d}} v^{(1)}_{\mathrm{u}} h^{(2)}_{\mathrm{u}} + w_{\mathrm{a}} v^{(4)}_{\mathrm{d}} v^{(1)}_{\mathrm{u}} v^{(2)}_{\mathrm{u}} + w^2_{\mathrm{p}} v^{(4)}_{\mathrm{d}} v^{(1)}_{\mathrm{d}} v^{(2)}_{\mathrm{d}} + w^2 v^{(4)}_{\mathrm{d}} v^{(1)}_{\mathrm{u}} s^{(2)} + v^{(4)}_{\mathrm{d}} h^{(1)}_{\mathrm{u}} s^{(2)} + v^{(4)}_{\mathrm{d}} s^{(1)} h^{(2)}_{\mathrm{u}} + v^{(4)}_{\mathrm{d}} s^{(1)} v^{(2)}_{\mathrm{u}} + v^{(4)}_{\mathrm{d}} s^{(1)} s^{(2)}, \tag{A4}$$

$$P^{(1)}_{\mathrm{h_u}} = w_{\mathrm{p}} v^{(4)}_{\mathrm{u}} v^{(1)}_{\mathrm{u}} h^{(2)}_{\mathrm{d}} + h^{(4)}_{\mathrm{u}} v^{(1)}_{\mathrm{u}} h^{(2)}_{\mathrm{d}} + v^{(4)}_{\mathrm{u}} h^{(1)}_{\mathrm{u}} h^{(2)}_{\mathrm{d}} + w_{\mathrm{a}} h^{(4)}_{\mathrm{u}} h^{(1)}_{\mathrm{u}} h^{(2)}_{\mathrm{d}} + w^2_{\mathrm{p}} h^{(4)}_{\mathrm{d}} h^{(1)}_{\mathrm{d}} h^{(2)}_{\mathrm{d}} + w^2 s^{(4)} v^{(1)}_{\mathrm{u}} h^{(2)}_{\mathrm{d}} + s^{(4)} h^{(1)}_{\mathrm{u}} h^{(2)}_{\mathrm{d}} + h^{(4)}_{\mathrm{u}} s^{(1)} h^{(2)}_{\mathrm{d}} + v^{(4)}_{\mathrm{u}} s^{(1)} h^{(2)}_{\mathrm{d}} + s^{(4)} s^{(1)} h^{(2)}_{\mathrm{d}}, \tag{A5}$$

$$P^{(2)}_i \text{ is obtained from } P^{(1)}_i \text{ by interchange } x^{(2)}_j \leftrightarrow x^{(1)}_j, \quad x^{(4)}_k \to x^{(3)}_k.$$

$$P^{(3)}_i \text{ is obtained from } P^{(1)}_i \text{ by interchange } x^{(2)}_j \leftrightarrow x^{(4)}_j, \quad x^{(1)}_k \to x^{(3)}_k.$$

$$P^{(4)}_i \text{ is obtained from } P^{(1)}_i \text{ by interchange } x^{(4)}_j \leftrightarrow x^{(1)}_j, \quad x^{(2)}_k \to x^{(3)}_k. \tag{A6}$$

We then calculate $Q^{(\alpha)}=\Sigma_i P^{(\alpha)}_i$ at each iteration step. Finally, the ratios are updated: $x^{(\alpha)^*}_j = P^{(\alpha)}_i / Q^{(\alpha)}$. This procedure is repeated until either a 1-cycle FP solution ($x^{(\alpha)^*}_j \to x^{(\alpha)}_j$) or 2 -cycle FP solution ($x^{(\alpha)^*}_{2k} \to x^{(\alpha)}_{2k}, x^{(\alpha)^*}_{2k+1} \to x^{(\alpha)}_{2k+1}$) is obtained.

2. General expression for ω

The total partition function can be calculated by two different methods depending on the center of the cactus. In the first method, the center is a square, as we have taken here in this work, and we take the product of four PPF's corresponding to four branches connected to the central square, and sum the product over all possibilities of the four sites of the central square. We compute the free energy, ω using the famous trick proposed in [53]. First we cut 12 branches on the level $m=1$. This leaves 5 squares. Next we construct 3 trees of smaller size connecting 4 branches and using one extra square at the center. At the end of this procedure one finds that exactly 4 sites are left out. Thus, the free energy per site ω is given by

$$\omega = \frac{1}{4} \ln\left(\frac{Z_0}{Z_1^3}\right), \tag{A7}$$

where Z_0 and Z_1 are the total partition functions of larger and smaller trees respectively. They, in turn, can be calculated in terms of the ratios only. The total partition function is given by the summation over all possible configurations in the central polygon:

$$Z_0 = \sum w^{(1234)}_{ijkl} Z^{(1)}_0(i) Z^{(2)}_0(j) Z^{(3)}_0(k) Z^{(4)}_0(l),$$

where $w^{(1234)}_{ijkl}$ are corresponding statistical weights. We can rewrite Z_0 in more simple form that utilizes (A1)–(A6):

$$Z_0 = B^{(2)}_0 B^{(3)}_0 B^{(4)}_0 (Z^{(1)}_0(\mathrm{v_u}) P^{(3)}_{0,\mathrm{v_d}} + Z^{(1)}_0(\mathrm{v_d}) P^{(3)}_{0,\mathrm{v_u}} + Z^{(1)}_0(\mathrm{h_u}) P^{(3)}_{0,\mathrm{h_d}} + Z^{(1)}_0(\mathrm{h_d}) P^{(3)}_{0,\mathrm{h_u}} + Z^{(1)}_0(\mathrm{s}) P^{(3)}_{0,\mathrm{s}} / \eta).$$

Thus, taking into account (24) and (26), we have

$$Z_0 = B^{(1)}_0 B^{(2)}_0 B^{(3)}_0 B^{(4)}_0 \widetilde{Q},$$

where

$$\widetilde{Q} = Q^{(3)} (v^{(1)'}_{\mathrm{u}} v^{(3)}_{\mathrm{d}} + v^{(1)'}_{\mathrm{d}} v^{(3)}_{\mathrm{u}} + h^{(1)'}_{\mathrm{u}} h^{(3)}_{\mathrm{d}} + h^{(1)'}_{\mathrm{d}} h^{(3)}_{\mathrm{u}} + s^{(1)'} s^{(3)} / \eta) = Q^{(3)} Q^{(13)}_0.$$

where the prime is important when the 2-cycle solution is of interest. On the other hand, Z_1 is given by

$$Z_1 = B^{(1)}_1 B^{(2)}_1 B^{(3)}_1 B^{(4)}_1 \widetilde{Q}',$$

where

$$\widetilde{Q}' = Q^{(3)'} Q^{(13)}_0.$$

Equation (A7) can be used when we write

$$Z_0 = (B^{(1)}_1 B^{(2)}_1 B^{(3)}_1 B^{(4)}_1)^3 Q^{(1)'} Q^{(2)'} Q^{(3)'} Q^{(4)'} \widetilde{Q}.$$

One notices the complexity of the calculations due to the index α and possible 2-cycle structure. We give also the expressions for the case when the index α is suppressed in the quantity. The total partition function for entire lattice is given by

$$Z_0 = B^4_0 Q Q_0,$$

where

$$Q_0 = 2 v_{\mathrm{u}} v_{\mathrm{d}} + 2 h_{\mathrm{u}} h_{\mathrm{d}}.$$

We now imagine taking out the 5 squares at the origin, which leaves behind 12 smaller branches of the cactus, from which we construct 3 smaller lattices by connecting 4 branches together each. The total PF of each of the smaller lattices is given by

$$Z_1 = B^4_1 Q Q_0,$$

so that we finally have

$$\omega = (1/2) \ln(Q/Q_0).$$

3. Densities

There are two types of densities that we are interested in: densities of some type of bonds or interaction contacts and densities of monomeric species. The former are densities as-

sociated with two neighboring sites and the latter are densities related to a single site. The density of bonds (contacts) of λ type, ϕ_λ, is the ratio $\phi_\lambda = N_\lambda / N$, where N_λ is number of such bonds (contacts) and N is the total number sites on the lattice. Similarly, $\phi_0 = N_0 / N$. We calculate these densities by multiplying Z_0 by the number of λ bonds (contacts) n_λ:

$$\phi_\lambda = \frac{\sum n_\lambda w_{ijkl}^{(1234)} Z_0^{(1)}(i) Z_0^{(2)}(j) Z_0^{(3)}(k) Z_0^{(4)}(l)}{2Z_0},$$

where $w_{ijkl}^{(1234)}$ are the weights associated with each configuration. The extra factor of 2 in the denominator is because there are 2 sites per square (a square has 4 sites, but each site is sheared by 4 squares). Hence

$$\phi_\lambda = \frac{\Phi_\lambda}{2\tilde{Q}},$$

where Φ_ξ is the fourth order polynomial in terms of ratios and $\tilde{Q}$. The exact expressions for Φ_c, Φ_p, Φ_a, that correspond to monomer-void, parallel-dimer, and axial contacts respectively are presented below. The simplest way to compute densities of monomeric species, e.g., the void density, ϕ_0, is to switch to the description that considers two central polygons as the tree origin:

$$\phi_0 = \frac{Z_{-1}^{(1)}(s) Z_0^{(3)}(s)}{\eta Z_0^{(13)}}.$$

Hence

$$\phi_0 = \frac{s^{(1)} s^{(3)}}{\eta Q_0^{(13)}}. \tag{A8}$$

On the other hand, the void density can also be calculated in more difficult way:

$$\phi_0 = \frac{\Phi_0}{4\tilde{Q}}.$$

The factor of 4 in the denominator is due to the fact that Φ_0 contains the factors representing numbers of voids for each configuration in the central square. At the same time, each site is sheared by two squares. In order to account for this, we divide by 4 instead. One could also define Φ_0 so that each void counts 1/2 in the numenator and divide by 2 in the denominator instead. We present here the expressions for Φ_c, Φ_p, Φ_a, that include the directional indices:

$$\begin{aligned}
\Phi_c = {} & 2w^2(s^{(1)}h_u^{(2)}v_d^{(3)}v_d^{(4)} + v_u^{(1)}s^{(2)}v_d^{(3)}v_d^{(4)} + h_u^{(1)}s^{(2)}v_d^{(3)}v_d^{(4)} + s^{(1)}s^{(2)}v_u^{(3)}s^{(4)} + v_u^{(1)}h_u^{(2)}v_u^{(3)}s^{(4)} + s^{(1)}v_u^{(2)}v_d^{(3)}v_d^{(4)} + s^{(1)}s^{(2)}v_d^{(3)}v_d^{(4)} \\
& + w_a w_p v_u^{(1)}v_u^{(2)}v_u^{(3)}s^{(4)} + s^{(1)}h_u^{(2)}v_u^{(3)}h_u^{(4)} + w_p h_u^{(1)}h_u^{(2)}v_u^{(3)}s^{(4)} + w_p h_u^{(1)}v_u^{(2)}v_u^{(3)}s^{(4)} + w_a s^{(1)}h_u^{(2)}v_u^{(3)}v_u^{(4)} + w_p s^{(1)}v_u^{(2)}v_u^{(3)}h_u^{(4)} \\
& + w_a w_p s^{(1)}v_a^{(2)}v_a^{(3)}v_a^{(4)} + w_a h_u^{(1)}s^{(2)}v_u^{(3)}h_u^{(4)} + s^{(1)}h_u^{(2)}v_u^{(3)}s^{(4)} + w_p s^{(1)}v_u^{(2)}v_u^{(3)}s^{(4)} + h_d^{(1)}s^{(2)}v_u^{(3)}h_d^{(4)} + v_d^{(1)}v_d^{(2)}v_u^{(3)}s^{(4)} \\
& + v_u^{(1)}s^{(2)}v_u^{(3)}h_u^{(4)} + w_p w_a v_u^{(1)}s^{(2)}v_u^{(3)}v_u^{(4)} + w_a h_u^{(1)}s^{(2)}v_u^{(3)}v_u^{(4)} + s^{(1)}s^{(2)}v_u^{(3)}h_u^{(4)} + w_a s^{(1)}s^{(2)}v_u^{(3)}v_u^{(4)} + s^{(1)}s^{(2)}h_u^{(3)}s^{(4)} \\
& + w_a s^{(1)}h_u^{(2)}h_u^{(3)}v_u^{(4)} + w_p s^{(1)}v_u^{(2)}h_u^{(3)}h_u^{(4)} + h_d^{(1)}s^{(2)}h_u^{(3)}h_d^{(4)} + v_d^{(1)}v_d^{(2)}h_u^{(3)}s^{(4)} + w_a w_p h_u^{(1)}h_u^{(2)}h_u^{(3)}s^{(4)} + v_u^{(1)}h_d^{(2)}h_d^{(3)}s^{(4)} \\
& + h_u^{(1)}h_d^{(2)}h_d^{(3)}s^{(4)} + s^{(1)}h_d^{(2)}h_d^{(3)}h_u^{(4)} + s^{(1)}h_d^{(2)}h_d^{(3)}v_u^{(4)} + s^{(1)}h_d^{(2)}h_d^{(3)}s^{(4)} + w_a w_p s^{(1)}h_u^{(2)}h_u^{(3)}h_u^{(4)} + s^{(1)}v_u^{(2)}h_u^{(3)}v_u^{(4)} \\
& + w_p v_u^{(1)}s^{(2)}h_u^{(3)}h_u^{(4)} + w_a w_p h_u^{(1)}s^{(2)}h_u^{(3)}h_u^{(4)} + w_p v_u^{(1)}s^{(2)}h_u^{(3)}v_u^{(4)} + h_u^{(1)}s^{(2)}h_u^{(3)}v_u^{(4)} + w_p s^{(1)}s^{(2)}h_u^{(3)}h_u^{(4)} + s^{(1)}s^{(2)}h_a^{(3)}v_a^{(4)} \\
& + w_a s^{(1)}h_u^{(2)}h_u^{(3)}s^{(4)} + s^{(1)}v_u^{(2)}h_u^{(3)}s^{(4)} + v_u^{(1)}h_u^{(2)}s^{(3)}h_u^{(4)} + h_u^{(1)}v_u^{(2)}s^{(3)}v_u^{(4)} + w_a v_u^{(1)}h_u^{(2)}h_u^{(3)}s^{(4)} + h_u^{(1)}v_u^{(2)}h_u^{(3)}s^{(4)} + w_a v_u^{(1)}v_u^{(2)}h_u^{(3)}s^{(4)} \\
& + h_d^{(1)}h_u^{(2)}s^{(3)}h_d^{(4)} + h_d^{(1)}v_u^{(2)}s^{(3)}h_d^{(4)} + v_d^{(1)}v_d^{(2)}s^{(3)}h_u^{(4)} + v_d^{(1)}v_d^{(2)}s^{(3)}v_u^{(4)} + w_a w_p h_u^{(1)}h_u^{(2)}s^{(3)}h_u^{(4)} + w_a w_p v_u^{(1)}v_u^{(2)}s^{(3)}v_u^{(4)} \\
& + v_u^{(1)}s^{(2)}s^{(3)}s^{(4)} + h_u^{(1)}s^{(2)}s^{(3)}s^{(4)} + w_p h_u^{(1)}h_u^{(2)}s^{(3)}s^{(4)} + v_u^{(1)}h_u^{(2)}s^{(3)}s^{(4)} + v_u^{(1)}s^{(2)}s^{(3)}h_u^{(4)} + w_a h_u^{(1)}s^{(2)}s^{(3)}h_u^{(4)} + s^{(1)}s^{(2)}s^{(3)}h_u^{(4)} \\
& + s^{(1)}h_u^{(2)}s^{(3)}s^{(4)} + h_d^{(1)}s^{(2)}s^{(3)}h_d^{(4)} + v_d^{(1)}v_d^{(2)}s^{(3)}s^{(4)} + h_u^{(1)}v_u^{(2)}s^{(3)}s^{(4)} + w_a v_u^{(1)}v_u^{(2)}s^{(3)}s^{(4)} + w_p v_u^{(1)}s^{(2)}s^{(3)}v_u^{(4)} + h_u^{(1)}s^{(2)}s^{(3)}v_u^{(4)} \\
& + s^{(1)}s^{(2)}s^{(3)}v_u^{(4)} + s^{(1)}v_u^{(2)}s^{(3)}s^{(4)} + w_p v_u^{(1)}h_u^{(2)}s^{(3)}v_u^{(4)} + w_p h_u^{(1)}h_u^{(2)}s^{(3)}v_u^{(4)} + w_a h_u^{(1)}v_u^{(2)}s^{(3)}h_u^{(4)} + w_a v_u^{(1)}v_u^{(2)}s^{(3)}h_u^{(4)} \\
& + 4w^4(v_u^{(1)}s^{(2)}v_u^{(3)}s^{(4)} + h_u^{(1)}s^{(2)}v_u^{(3)}s^{(4)} + v_u^{(1)}s^{(2)}h_u^{(3)}s^{(4)} + h_u^{(1)}s^{(2)}h_u^{(3)}s^{(4)} + s^{(1)}h_u^{(2)}s^{(3)}h_u^{(4)} + s^{(1)}v_u^{(2)}s^{(3)}v_u^{(4)} + s^{(1)}h_u^{(2)}s^{(3)}v_u^{(4)} \\
& + s^{(1)}v_u^{(2)}s^{(3)}h_u^{(4)}),
\end{aligned}$$

$$\begin{aligned}
\Phi_p = {} & (w^2 w_a h_u^{(1)}s^{(2)}h_u^{(3)}h_u^{(4)} + w^2 v_u^{(1)}s^{(2)}h_u^{(3)}v_u^{(4)} + w^2 v_u^{(1)}s^{(2)}h_u^{(3)}h_u^{(4)} + w^2 w_a s^{(1)}v_u^{(2)}v_u^{(3)}v_u^{(4)} + w^2 w_a s^{(1)}h_u^{(2)}h_u^{(3)}h_u^{(4)} \\
& + w^2 w_a h_u^{(1)}h_u^{(2)}h_u^{(3)}s^{(4)} + w^2 s^{(1)}s^{(2)}h_u^{(3)}h_u^{(4)} + w^2 s^{(1)}v_u^{(2)}h_u^{(3)}h_u^{(4)} + w_a v_u^{(1)}h_u^{(2)}h_u^{(3)}v_u^{(4)} + w_a h_u^{(1)}h_u^{(2)}h_u^{(3)}v_u^{(4)} + w_a h_u^{(1)}v_u^{(2)}h_u^{(3)}h_u^{(4)} \\
& + w_a v_u^{(1)}v_u^{(2)}h_u^{(3)}h_u^{(4)} + w_a v_u^{(1)}v_u^{(2)}h_u^{(3)}v_u^{(4)} + v_d^{(1)}v_d^{(2)}h_u^{(3)}h_u^{(4)} + w_a v_u^{(1)}h_u^{(2)}h_u^{(3)}h_u^{(4)} + w^2 v_u^{(1)}s^{(2)}s^{(3)}v_u^{(4)} + w^2 h_u^{(1)}h_u^{(2)}s^{(3)}s^{(4)} \\
& + v_u^{(1)}h_d^{(2)}h_d^{(3)}v_u^{(4)} + w_a h_u^{(1)}v_u^{(2)}v_u^{(3)}h_u^{(4)} + w_a v_u^{(1)}v_u^{(2)}v_u^{(3)}h_u^{(4)} + w_a h_u^{(1)}h_u^{(2)}v_u^{(3)}h_u^{(4)} + w_a h_u^{(1)}v_u^{(2)}v_u^{(3)}v_u^{(4)} + h_d^{(1)}v_u^{(2)}v_u^{(3)}h_d^{(4)} \\
& + w_a v_u^{(1)}h_u^{(2)}v_u^{(3)}v_u^{(4)} + w^2 w_a v_u^{(1)}v_u^{(2)}v_u^{(3)}s^{(4)} + w^2 h_u^{(1)}v_u^{(2)}v_u^{(3)}s^{(4)} + w^2 h_u^{(1)}h_u^{(2)}v_u^{(3)}s^{(4)} + w^2 s^{(1)}v_u^{(2)}v_u^{(3)}s^{(4)} + w^2 s^{(1)}v_u^{(2)}v_u^{(3)}h_u^{(4)} \\
& + h_u^{(1)}h_u^{(2)}v_d^{(3)}v_d^{(4)} + w_a h_u^{(1)}h_u^{(2)}v_u^{(3)}v_u^{(4)} + w^2 v_u^{(1)}h_u^{(2)}s^{(3)}v_u^{(4)} + w^2 w_a h_u^{(1)}h_u^{(2)}s^{(3)}h_u^{(4)} + w^2 w_a v_u^{(1)}v_u^{(2)}s^{(3)}v_u^{(4)} + w^2 h_u^{(1)}h_u^{(2)}s^{(3)}v_u^{(4)} \\
& + w^2 w_a v_u^{(1)}s^{(2)}v_u^{(3)}v_u^{(4)})w_p/2 + (w_a^2 h_u^{(1)}h_u^{(2)}h_u^{(3)}h_u^{(4)} + w_a^2 v_u^{(1)}v_u^{(2)}v_u^{(3)}v_u^{(4)})w_p^2 + (h_d^{(1)}h_d^{(2)}h_d^{(3)}h_d^{(4)} + v_d^{(1)}v_d^{(2)}v_d^{(3)}v_d^{(4)})w_p^2,
\end{aligned}$$

$$\Phi_a = w_a(w_p h_u^{(1)} h_u^{(2)} v_u^{(3)} h_u^{(4)} + v_u^{(1)} v_u^{(2)} v_d^{(3)} v_d^{(4)} + w_p v_u^{(1)} h_u^{(2)} v_u^{(3)} v_u^{(4)} + w_p h_u^{(1)} h_u^{(2)} v_u^{(3)} v_u^{(4)} + w_p h_u^{(1)} v_u^{(2)} v_u^{(3)} h_u^{(4)} + w_p v_u^{(1)} v_u^{(2)} v_u^{(3)} h_u^{(4)}$$
$$+ w_p h_u^{(1)} v_u^{(2)} v_u^{(3)} v_u^{(4)} + w^2 w_p v_u^{(1)} v_u^{(2)} v_u^{(3)} s^{(4)} + w^2 s^{(1)} h_u^{(2)} v_u^{(3)} v_u^{(4)} + w^2 w_p s^{(1)} v_u^{(2)} v_u^{(3)} v_u^{(4)} + w^2 h_u^{(1)} s^{(2)} v_u^{(3)} h_u^{(4)} + v_d^{(1)} v_d^{(2)} v_u^{(3)} v_u^{(4)}$$
$$+ w^2 w_p v_u^{(1)} s^{(2)} v_u^{(3)} v_u^{(4)} + w^2 h_u^{(1)} s^{(2)} v_u^{(3)} v_u^{(4)} + w^2 s^{(1)} s^{(2)} v_u^{(3)} v_u^{(4)} + h_u^{(1)} h_d^{(2)} h_d^{(3)} h_u^{(4)} + w_p v_u^{(1)} v_u^{(2)} h_u^{(3)} v_u^{(4)} + w_p v_u^{(1)} h_u^{(2)} h_u^{(3)} h_u^{(4)}$$
$$+ w_p v_u^{(1)} h_u^{(2)} h_u^{(3)} v_u^{(4)} + w_p h_u^{(1)} h_u^{(2)} h_u^{(3)} v_u^{(4)} + w_p h_u^{(1)} v_u^{(2)} h_u^{(3)} h_u^{(4)} + w^2 w_p h_u^{(1)} h_u^{(2)} h_u^{(3)} s^{(4)} + w_p v_u^{(1)} v_u^{(2)} h_u^{(3)} h_u^{(4)} + h_d^{(1)} h_u^{(2)} h_u^{(3)} h_d^{(4)}$$
$$+ w^2 s^{(1)} h_u^{(2)} h_u^{(3)} v_u^{(4)} + w^2 v_u^{(1)} v_u^{(2)} s^{(3)} s^{(4)} + w^2 h_u^{(1)} v_u^{(2)} s^{(3)} h_u^{(4)} + w^2 v_u^{(1)} v_u^{(2)} s^{(3)} h_u^{(4)} + w^2 w_p h_u^{(1)} h_u^{(2)} s^{(3)} h_u^{(4)} + w^2 w_p v_u^{(1)} v_u^{(2)} s^{(3)} v_u^{(4)}$$
$$+ w^2 v_u^{(1)} h_u^{(2)} h_u^{(3)} s^{(4)} + w^2 v_u^{(1)} v_u^{(2)} h_u^{(3)} s^{(4)} + w^2 w_p s^{(1)} h_u^{(2)} h_u^{(3)} h_u^{(4)} + w^2 w_p h_u^{(1)} s^{(2)} h_u^{(3)} h_u^{(4)} + w^2 s^{(1)} h_u^{(2)} h_u^{(3)} s^{(4)} + w^2 h_u^{(1)} s^{(2)} s^{(3)} h_u^{(4)})$$
$$+ 2 w_a^2 w_p^2 (h_u^{(1)} h_u^{(2)} h_u^{(3)} h_u^{(4)} + v_u^{(1)} v_u^{(2)} v_u^{(3)} v_u^{(4)}).$$

[1] W. Kauzmann, Chem. Rev. (Washington, D.C.) **43**, 219 (1948).

[2] *The Glass Transition and the Nature of the Glassy State*, edited by M. Goldstein and R. Simha [Ann. N.Y. Acad. Sci. 279 (1976)].

[3] M. D. Ediger, C. A. Angell, and S. R. Nagel, J. Phys. Chem. **100**, 13200 (1996).

[4] P. G. Debenedetti, *Metastable Liquids: Concepts and Principles* (Princeton University Press, Princeton, NJ, 1996).

[5] O. Mishima, L. D. Calvert, and E. Whalley, Nature (London) **314**, 76 (1985); O. Mishima, J. Chem. Phys. **100**, 5910 (1994).

[6] P. H. Poole, F. Sciortino, U. Essmann, and H. E. Stanley, Nature (London) **360**, 324 (1992); F. Sciortino, P. H. Poole, U. Essmann, and H. E. Stanley, Phys. Rev. E **55**, 727 (1997).

[7] W. Gotze, in *Liquids, Freezing and the Glass Transition*, edited by J. P. Haasma, D. Levesque, and J. Zinn-Justin (North-Holland, Amsterdam, 1991), p. 287; W. Götze and L. Sjögren, Rep. Prog. Phys. **55**, 241 (1992).

[8] P. D. Gujrati and A. Corsi, Phys. Rev. Lett. **87**, 025701 (2001).

[9] A. Corsi and P. D. Gujrati, Phys. Rev. E **68**, 031502 (2003); cond-mat/0308555.

[10] P. D. Gujrati, S. S. Rane, and A. Corsi, Phys. Rev. E **67**, 052501 (2003).

[11] For a macroscopic system, the contribution due to $\ln dE$ (or due to $\ln dP$; see later) to the entropy is negligible, and will be neglected in the following. Once we discretize the space, as we discuss later in Sec. II, this issue is no longer relevant.

[12] Entropy being less than a positive value, no matter how small, *cannot* be as fundamental an entropy crisis requirement $S<0$ to argue for an ideal glass transition. For example, liquid helium shows no glass transition when its entropy becomes equal to such a small positive value. Thus, we will adhere to $S<0$ as the most fundamental requirement for the entropy crisis. This also rules out using the excess entropy $S_{ex}(T)=S_{T\text{-}SCL}(T)-S_{T\text{-}CR}(T)$, used by Kauzmann and various other authors, as a signal of an entropy crisis when it becomes negative, since thermodynamics itself does not rule out the possibility that the total CR entropy $S_{T\text{-}CR}(T)$ can be greater than the total liquid (SCL) entropy as seen recently [8–10]. Liquid He also has the property that its CR phase can have higher entropy than the liquid phase at low temperatures. Thus, $S_{ex}(T)<0$ does not pose any thermodynamic problem of stability or reality, and we will not use its becoming negative as the signal for any entropy crisis although it is commonly done; rather, we will use the condition $S<0$ as the criterion for the entropy crisis. The temperature at which $S=0$ is called here the ideal glass transition temperature or the Kauzmann temperature T_K, even though the latter is traditionally identified as the temperature where $S_{ex}(T)$ vanishes; see also the discussion in Sec. II C.

[13] P. D. Gujrati, cond-mat/0309143.

[14] B. Derrida, Phys. Rev. B **24**, 2613 (1981).

[15] P. D. Gujrati, J. Phys. A **13**, L437 (1980); P. D. Gujrati and M. Goldstein, J. Chem. Phys. **74**, 2596 (1981); P. D. Gujrati, J. Stat. Phys. **28**, 241 (1982).

[16] J. H. Gibbs and E. A. DiMarzio, J. Chem. Phys. **28**, 373 (1958).

[17] E. A. Di Marzio and A. J. Yang, J. Res. Natl. Inst. Stand. Technol. **102**, 135 (1997).

[18] L. D. Landau and E. M. Lifshitz, *Statistical Physics, Vol. 1*, third ed. (Pergamon Press, Oxford, 1986).

[19] D. Ruelle, Physica A **113A**, 619 (1982).

[20] F. Sciortino, W. Kob, and P. Tartaglia, Phys. Rev. Lett. **83**, 3214 (1999); B. Coluzzi, G. Parisi, and P. Verrocchio, *ibid.* **84**, 306 (2000); L. Santen and W. Krauth, Nature (London) **405**, 550 (2000).

[21] C. A. Angell, Science **267**, 1924 (1995). P. H. Poole, T. Grande, C. A. Angell, and P. F. McMillan, Science **275**, 322 (1997).

[22] E. W. Fischer, Physica A **210**, 183 (1993).

[23] H. Tanaka, Phys. Rev. E **62**, 6968 (2000).

[24] D. R. Nelson, Phys. Rev. B **28**, 5515 (1983).

[25] P. G. Debenedetti and F. H. Stillinger, Nature (London) **410**, 259 (2001).

[26] T. R. Kirkpatrick and P. G. Wolynes, Phys. Rev. A **35**, 3072 (1987); T. R. Kirkpatrick, D. Thirumalai, and P. G. Wolynes, Phys. Rev. A **40**, 1045 (1989).

[27] C. A. Angell, J. Non-Cryst. Solids **131–133**, 13 (1991).

[28] (a) S. Franz and G. Parisi, Phys. Rev. Lett. **79**, 2486 (1997); (b) L. Angelani, G. Parisi, G. Ruocco, and G. Viliani, Phys. Rev. Lett. **81**, 4648 (1998); (c) M. Mézard and G. Parisi, Phys. Rev. Lett. **82**, 747 (1999); (d) B. Coluzzi, G. Parisi, and P. Verrocchio, Phys. Rev. Lett. **84**, 306 (2000).

[29] D. Kivelson and G. Tarjus, J. Chem. Phys. **109**, 5481 (1998).

[30] (a) S. Sastry, P. G. Debenedetti, and F. H. Stillinger, Nature (London) **393**, 554 (1998); (b) S. Sastry, Phys. Rev. Lett. **85**, 590 (2000).

[31] (a) M. H. Cohen and D. Turnbull, J. Chem. Phys. **31**, 1164

(1959); (b) M. H. Cohen and G. S. Grest, Phys. Rev. B **20**, 1077 (1979).
[32] (a) Mukesh Chhajer and P. D. Gujrati, J. Chem. Phys. **109**, 9022 (1998); (b) S. Rane and P. D. Gujrati, Phys. Rev. E **64**, 011801 (2001).
[33] A. K. Doolittle, J. Appl. Phys. **22**, 1471 (1951).
[34] G. Adams and J. H. Gibbs, J. Chem. Phys. **43**, 139 (1965).
[35] G. P. Johari, J. Chem. Phys. **113**, 751 (2000).
[36] M. Pyda and B. Wunderlich, J. Polym. Sci., Part B: Polym. Phys. **40**, 1245 (2002).
[37] F. H. Stillinger, J. Chem. Phys. **88**, 7818 (1988).
[38] D. Kievelson, S. A. Kivelson, X. Zhao, Z. Nussinov, and G. Tarjus, Physica A **219**, 27 (1995).
[39] C. A. Angell, J. Res. Natl. Inst. Stand. Technol. **102**, 171 (1997).
[40] P. D. Gujrati and M. Goldstein, J. Phys. Chem. **84**, 859 (1980), and references therein.
[41] M. Toda, R. Kubo, and N. Saito, *Statistical Physics I* (Springer-Verlag, Berlin, 1978).
[42] C. J. Thompson, *Classical Equilibrium Statistical Mechanics* (Clarendon Press, Oxford, 1988).
[43] A. L. Fetter and J. D. Walecka, *Theoretical Mechanics of Particles and Continua* (McGraw-Hill, New York, 1980).
[44] E. A. DiMarzio, in *XXIII International Congress of Pure and Applied Chemistry* (Butterworths, London, 1971), Vol. 8.
[45] R. J. Speedy, J. Phys. Chem. B **103**, 4060 (1999).
[46] P. D. Gujrati, cond-mat/0412528; cond-mat/0412735.
[47] O. Penrose and J. L. Lebowitz, in *Fluctuation Phenomena*, edited by E. W. Montroll and J. L. Lebowitz (North-Holland, Amsterdam, 1979).
[48] P. D. Gujrati, cond-mat/0412757.
[49] P. D. Gujrati, J. Chem. Phys. **112**, 4806 (1994).
[50] P. W. Anderson, Science **235**, 278 (1987).
[51] J. L. Monroe, Phys. Rev. E **64**, 016126 (2001).
[52] P. D. Gujrati, J. Chem. Phys. **108**, 6952 (1994).
[53] P. D. Gujrati, Phys. Rev. Lett. **74**, 809 (1995).
[54] F. Semerianiv, Ph.D. dissertation, The University of Akron, 2004.
[55] P. W. Kasteleyn, Physica (Amsterdam) **27**, 1209 (1961).
[56] M. E. Fisher, Phys. Rev. **124**, 1664 (1961).
[57] T. S. Chang, Proc. R. Soc. London, Ser. A **169**, 512 (1939).
[58] D. S. Rokhsar and S. A. Kivelson, Phys. Rev. Lett. **61**, 2376 (1988).
[59] N. Read and S. Sachdev, Nucl. Phys. B **316**, 609 (1989); T. Dombre and G. Kotliar, Phys. Rev. B **39**, 855 (1989).
[60] R. Moessner, S. L. Sondhi, and E. Fradkin, Phys. Rev. B **65**, 024504 (2001).